

T-2069

EFFECT OF JET PERFORATION
ON FOAM CEMENT

by

Khaled Chekiri

ARTHUR LAKES LERRAW
COLORADO SCHOOL OF MINES
GOLDEN, COLORADO 80401

ProQuest Number: 11016474

All rights reserved

INFORMATION TO ALL USERS

The quality of this reproduction is dependent upon the quality of the copy submitted.

In the unlikely event that the author did not send a complete manuscript and there are missing pages, these will be noted. Also, if material had to be removed, a note will indicate the deletion.



ProQuest 11016474

Published by ProQuest LLC (2019). Copyright of the Dissertation is held by the Author.

All rights reserved.

This work is protected against unauthorized copying under Title 17, United States Code
Microform Edition © ProQuest LLC.

ProQuest LLC.
789 East Eisenhower Parkway
P.O. Box 1346
Ann Arbor, MI 48106 – 1346

A Thesis submitted to the Faculty and the Board of Trustees of Colorado School of Mines in partial fulfillment of the requirements for the degree of Master of Science in Petroleum Engineering.

Signed: *H. Chekin*
Student

Golden, Colorado

Date: 5/80, 1978

Approved: *Am Bass*
Thesis Advisor and
Head of Department

Golden, Colorado

Date: 5/10/, 1978

ABSTRACT

Twelve foam cement samples, with qualities ranging from zero to fifty percent are jet perforated. Foam cement was generated in the laboratory by agitating cement slurry, surfactant and air in a closed container; the agitation was developed by a paint shaker. For every quality, two cement slurry compositions were used: one with thirty percent silica flour, the other without. Foam cement cured in 3-ft-long, 4 1/2-in. inside diameter casing sections at room temperature and atmospheric pressure. The samples were perforated with a 4 in. Jumbo Jet charge then longitudinally cut along the perforation. The perforations are described and schematically illustrated. Damage to cement is reported and discussed. Plots of entrance hole diameter and jet penetration versus Quality are presented.

TABLE OF CONTENTS

ABSTRACT.	iii
TABLE OF CONTENTS.	iv
LIST OF FIGURES.	vi
LIST OF TABLES	ix
ACKNOWLEDGEMENT.	xi
INTRODUCTION	1
LITERATURE SURVEY.	3
General	3
Emulsions	4
Foam Cement	8
Jet Perforation	9
Summary of Previous Work and Its Relation to this Study.	13
Definitions	14
EXPERIMENTAL PROCEDURE	15
Paint Shaker.	15
Preliminary Tests	17
Sample Preparation.	18

Perforation Test.	20
RESULTS AND DISCUSSION.	21
Mixing.	21
Adhesion to Casing.	22
Perforation	23
Conclusions	28
FIGURES	29-75
TABLES.	76-93
REFERENCES	94
APPENDIX A.	96
APPENDIX B	98

LIST OF FIGURES

1. Schematic Form of the Curve of Total Potential Energy.	29
2. Permeability of Foam Cement	30
3. Compressive Strength of Foam Cement	31
4. Compressive Strength of Foam Cement-Silica Flour.	32
5. Tensile Strength of Foam Cement-Silica Flour.	33
6. Tensile Strength versus Mixing Pressure	34
7. Foam Cement Compressive Strength Versus Porosity of Set Cement, 28 Days, 140°F.	35
8. Foam Cement Tensile Strength Versus Porosity of Set Cement, 28 Days, 140°F.	36
9. Detonation Stages of a Typical Shaped Charge.	37
10. Cross Section Showing the Collapse Process in a Conical Liner.	38
11. Bullet, Jet and Hydraulic Perforator Performance	39
12. Jet Penetration vs. Formation Strength.	40
13. Concrete Test Target.	41
14. Foam Cement Injection System.	42

15. Segregation along a 3 in. Sample.	43
16. A Paint Shaker.	44
17a. Paint Shaker (Schematic)	45
17b. Schematic Representation of a Paint Shaker's Movement	46
18. Typical Batch Homogeneity Analysis.	47
19. Injection System into a Plexiglass Tube.	48
20. Typical Foam Stability Analysis	49
21. Ultimate Segregation.	50
22. Minimum Surfactant Concentration vs. Quality	51
23. Sample Perforation Setup.	52
24. Adhesion of Foam Cement to the Pipe	53
25. Shear Bonding Strength versus Compressive Strength.	54
26. Cross Sections, Low Quality Samples	55
27. Cross Sections, High Quality Samples.	56
28. Effect of Steel Plate Thickness on Perforation Diameter.	57
29. Entrance Hole-Size versus Quality	58
30. Bottom Plate of Sample #1	59
31. Jet Penetration versus Quality.	60
32. Cross Section, Neat Cement.	61

33. Cross Section, Fifty percent Quality.	62
34. Probable Stress-Strain Curves for Neat Cement (a) and Foam Cement (b)	63
35. Cross Section, Sample #1.	64
36. Cross Section, Sample #2.	65
37. Cross Section, Sample #3.	66
38. Cross Section, Sample #4.	67
39. Cross Section, Sample #5.	68
40. Cross Section, Sample #6.	69
41. Cross Section, Sample #7.	70
42. Cross Section, Sample #8.	71
43. Cross Section, Sample #9.	72
44. Cross Section, Sample #10	73
45. Cross Section, Sample #11	74
46. Cross Section, Sample #12	75

LIST OF TABLES

1. Sieve Analysis.	76
2. Typical Non-Homogeneous Batch	77
3. Typical Homogeneous Batch	78
4. Typical Unstable Foam	79
5. Typical Stable Foam	80
6. Homogeneity Check on Foam Cement Samples, 50% Quality.	81
7. Homogeneity Check on Foam Cement Samples, 50% Quality.	82
8. Homogeneity Check on Foam Cement Samples, 40% Quality.	83
9. Homogeneity Check on Foam Cement Samples, 40% Quality.	84
10. Homogeneity Check on Foam Cement Samples, 30% Quality.	85
11. Homogeneity Check on Foam Cement Samples, 30% Quality.	86
12. Homogeneity Check on Foam Cement Samples, 20% Quality.	87
13. Homogeneity Check on Foam Cement Samples, 20% Quality.	88

14. Homogeneity Check on Foam Cement Samples, 10% Quality.	89
15. Homogeneity Check on Foam Cement Samples, 10% Quality.	90
16. Homogeneity Check on Foam Cement Samples, 0% Quality	91
17. Homogeneity Check on Foam Cement Samples, 0% Quality	92
18. Summary of Target Samples Conditions.	93

ACKNOWLEDGEMENT

The author wishes to express his appreciation to Dr. D.M. Bass who acted as research advisor throughout this study, to Dr. B.J. Mitchell whose constructive criticism was invaluable. In addition, appreciation is extended to Dr. D.W. Hilchie and Prof. D. Dickinson who patiently read and criticized the manuscript for content and clarity.

Many thanks are due to Dresser Atlas for graciously carrying out the perforation tests; to the Amoco Production Company, Chevron-West, Chevron-Oil Field Research Company, El Paso Natural Gas Company, Exxon and Getty for their financial support; to Jim Boze for his help in solving the numerous mechanical problems during the experiment.

Finally I wish to thank the Algerian Oil Company, SONATRACH, for its generous assistance throughout my graduate studies in the United States.

INTRODUCTION

Discovery of Portland cement is credited to an English bricklayer, Joseph Aspdin, who in 1824 was issued a patent by the British government for the production of Portland cement (1, 2). Future developments in the manufacturing of Portland cement resulted in its wide use in the oil industry.

With the advent of basic cements, additives were commonly used to affect the characteristics of cement slurries. In many cases, the use of chemicals is necessary. Many formations, for example, will not support long cement columns with densities exceeding fifteen pounds per gallon. Low density slurries were sought and low weight additives developed.

The density of a cement slurry can also be lowered by the introduction of gas bubbles. Foam cement consists of a continuous cement phase and a discontinuous gas phase in the form of bubbles. Foam cement found its first use in the construction industry, primarily because of its insulating properties. The strength of such a material, however, was far below building requirements; its use remains restricted to roofs and wall panels (3).

A characteristic of foam cement is its quality. Quality of foam cement is the ratio of the gas volume to the total volume. In this study, quality will be assumed equal to porosity; i.e., shrinkage, expansion or microporosity effects were not considered.

In the oil industry, foam cement can have many uses. Because of the low density, the adequate compressive strengths, the low permeability, and the good insulating properties, foam cements can be used in a routine primary cement job to:

- Bond and support the casing.
- Restrict fluid movement between different formations.

Foam cements are perfect for some special jobs like:

- Cementing formations subject to fracture.
- Cementing large holes.

The most popular method for establishing communication between a cemented formation and production string is jet perforating. The first objective in jet perforating is to achieve the deepest penetration possible without damaging either the pipe or the cement sheath. The effects of jet perforating on foam cement are investigated in this study. Twelve foam cement cores were perforated. Damage to cement, hole size and depth of penetration are reported. Other noteworthy observations about foam cement are also presented.

LITERATURE SURVEY

The obtaining of a long column of homogenous foam cement was the first objective of this study.

General

Practically no physical law relative to foam cement formation or stability is found in the literature. Most studies are restricted to the case of two-phase systems. The principal physical effects considered in these studies are:

- (a) Capillary pressure (4):

$$P_g = \frac{4\gamma}{r} + P_s$$

where

P_g = pressure within a gas bubble

P_s = pressure within the slurry

γ = interfacial tension

r = radius of bubble

- (b) Gas law:

$$\Delta V = NRT\Delta(Z/P)$$

where

ΔV = a change in slurry volume

$\Delta(Z/P)$ = a change in the ratio of gas deviation

factor over pressure

N = moles of gas

R = gas constant

T = absolute temperature

(c) Stoke's law:

$$v = \frac{2gr^2(\rho_2 - \rho_1)}{9\eta_2}$$

where

ρ_1 = density of the bubble

ρ_2 = density of the continuous phase

η_2 = viscosity of the continuous phase

v = velocity of the bubble

For gas liquid systems, the equation reduces to

$$v = \frac{gr^2\rho_2}{3\eta_2}$$

Since $\rho_2 \gg \rho_1$

Emulsions

A.M. Al-Mashat (6) recognized the similarity between emulsions and foam cement. He acknowledged the possibility that theories derived for emulsions might be applied for foam cement.

Most emulsions are formed either by orifice mixing or high shear.

Orifice mixing consists of injecting one liquid phase in another. The velocity of flow is an important factor in the efficiency of the mixing. Richardson (7) reported that liquid breakup of the dispersed phase is controlled by inertial and viscous forces. A critical jet

velocity, V_0 , is required for good mixing.

This velocity is obtained from Ohnesorge's relation as reported by Becher (8).

$$\eta_1 / (\rho_1 \gamma D)^{1/2} = 2,000 (\eta_1 / V_0 \rho_1 D)^{4/3}$$

where

D = the nozzle diameter

ρ_1 = density of dispersed phase

η_1 = viscosity of dispersed phase

γ = interfacial tension

The other method of producing an emulsion is to divide the relatively large particles of the dispersed phase into smaller ones by subjecting them to high shear conditions. Rumscheidt and Mason (9) (1960) studied the deformation and breakup of fluid drops under conditions of shear. They extended the work of Taylor (10) (1932), where he defines E as the ratio of the viscous forces over the surface tension forces. The authors show that the critical deformation above which the droplet will burst is given by:

$$Ff(P) = E = 1/2$$

where

$$F = Gr\eta_2 / \gamma$$

$$f(p) = (19p + 16) / (16p + 16)$$

$$p = \eta_1 / \eta_2$$

In these relations,

G = shear rate

r = radius of the undeformed drop

η_1 = viscosity of the drop

η_2 = viscosity of the continuous phase

γ = interfacial tension

Drop or bubble size and size distribution have been recognized as very critical factors in the stability of an emulsion or a foam. The smaller the drop or bubble size and the narrower the distribution, the more stable is the emulsion. These conditions are necessary for stability but are not sufficient to guarantee it. To achieve a small drop size, the work necessary to create an emulsion will be stored in the system as potential energy. This constitutes a considerable degree of thermodynamic instability, which is reduced by adding surfactants to the system to lower the surface tension between the continuous and the dispersed phases.

The possibility that electrical effects might be of considerable importance on the stability of foam have been recognized by many authors. In the electric theory, frequently called D.L.V.O.'S theory after Derjaguin, Landau, Verway and Overbeek (12, 13), the simple pair wise addition of the potential energy of electrostatic repulsion (V_r) and the Van Der Waal attraction (V_a) is assumed.

The total potential energy of interaction is:

$$V_t = V_a + V_r$$

Fig. 1 shows the type of curve obtained by the above summation.

Emulsions were found to be stabilized by finely divided solids (14). An elaborate study of emulsions stabilized by hydroxide of metals was carried out by Mukerjee & Scrivastava (15). One of the pertinent findings related to the present study was the apparent relationship between stability and the valence of the metal ion. Emulsions stabilized with hydroxides of valence greater or equal to three were very stable.

In 1973, Bikerman (16), speaking about froth floatation (a procedure to separate minerals from unneeded waste), explained how solid particles become attached to bubbles and concluded that three-phase foams are less affected by film drainage than two-phase systems.

Foam Cement

The main characteristic of oil well cements is their strength. All studies related to foam cements have focused on this important property.

The first study concerning foam cement's use in the oil industry was completed by C.A. Aldrich (17) in 1974. Two important conclusions were drawn. First, that foam cement has adequate strengths and no permeability at qualities below fifty percent. The second is that when foam cement quality exceeds fifty-one percent, there is a tremendous increase in permeability. Figs. 2 and 3 summarize Aldrich findings.

In 1976, J.P. Slattery (18) studied the strength and setting time of foam cement with various additives. His study showed that early strengths (72 hours) of foam cement are sufficient for oil well applications, Figs. 4 and 5.

That same year, a paper by V.P. Detkov and A.K. Sabrizyanov (19) appeared in the Russian literature. The authors studied the strength of foam cement at different mixing pressures. The qualities tested were limited to only ten and fifteen percent. They concluded that tensile strength is highly affected by mixing pressures. At 10 Kg/cm² (150 psi) mixing pressure, ten percent quality cement has a tensile strength of 14 Kg/cm² (200 psi). At 100 Kg/cm² (1500 psi) mixing pressure, the tensile strength is increased to 18 Kg/cm² (260 psi), Fig. 6; this figure shows also that at high mixing pressures (curve 1) the strength of high quality cement approaches that of lower quality (curve 2).

A later study carried out by E. Pakbaz (20) determined compressive strengths and tensile strengths of cements with various additives. Curing time and temperature effects on cement strengths were studied. Figs. 7 and 8 show the tensile and compressive strengths of foam cement and silica flour for twenty-eight days curing time.

Jet Perforation

For most well completions, casing is set through the producing zone, cemented and perforated for production.

Two types of perforating guns are available: bullet and shaped charges.

The use of bullets has steadily declined since the introduction of the shaped charge perforator in the late 1940's. A jet perforator consists of the following, Fig. 9a.

1. The booster or primer is an explosive pellet that increases the speed of detonation. Its physical form controls the shape of the detonation wave front. The booster is detonated using a prima cord.

2. The explosive charge may consist of any explosive material but detonation speed, availability and cleanliness of the explosive charge limit the choice. The explosive force must be sufficient to obtain the desired penetration and hole size without damaging the gun or the casing.

3. The liner is the most important and most influential component of the shaped charge assembly. Any variation in its dimensions or shape has a great effect on the perforator's performance. The liner

is a thin, usually cone-shaped metal sheet (mostly copper and zinc), that gives the perforating jet sufficient density to penetrate a material.

The detonation stages of a typical shaped charge perforator are illustrated in Figs. 5b through 5e, and best described by the following paragraphs selected from "Perforating Technology"(21).

"In Fig. [9b] the wave front has progressed through the explosive's solid body far enough to attain maximum velocity. At this point, for example, the velocity in a blended cyclonite charge would be in the order of 20,000 feet per second.

When the wave front strikes the apex of the liner, tremendous pressures start to collapse the liner on its own axis. Because the pressures are so far beyond the yield strength of any metal used in the liner, the metal acts as a perfect fluid. As the liner material converges at the axis, it is squeezed by peripheral pressure at the plane of the wave front. A portion will move forward; a portion will move rearward. See Fig. [9c].

The relative motions of the fluidized metal can be delineated by the centerline of the liner wall. Material on the outer or explosive side of this line will move to the rear and form a slug. Material on the inner side will enter the jet stream and move forward. At this point, the jet is just forming and can be disrupted.

This characteristic permits fail-safe shipping of shaped charges. Solid matter is placed in the cone at the apex, and will prevent the forming of the jet even though detonation occurs.

Fig. [9d] shows the wave front about half-way down the cone. The slug has been squirted farther back with respect to the wave front and the jet has lengthened. By this time, the jet stream has reached its highest velocity. It can reach twice the velocity of the explosive charge's detonation. A jet stream of that velocity produces impact forces well beyond the yield strength of any metal or rock. The pressure has been estimated to be about 6,000,000 psi. The forward portion of the jet will have a velocity up to 25,000 feet per second, while the slug at the rear of the jet will have a forward speed of about 3,000 feet per second. The difference in speed

of the forward and back part of the jet accounts for the lengthening of the jet. In Fig. [9c], the wave front has passed the base of the cone. The jet has extended to its full length. All the material in the cone has been injected either into the jet stream or the slug".

The first detailed explanation of the jet charge process described above appeared in unclassified literature in 1948. In a paper by Birkoff, et al. (22), mathematical steady state theories based upon classical hydrodynamics were used to describe the various features of jet perforation.

Four years later, Pugh et al. (23), noticed that by neglecting the steady state assumption, properties of the slug could be explained. They assumed that the collapse velocity was not identical for all elements of the liner and, therefore, the contour of the collapsing cone does not remain conical but takes on the contour illustrated in Fig. 10. Formulae were derived to quantitatively evaluate both jet and slug (velocity and mass) as well as the shape of the collapsing liner at any instant of time.

According to the hydrodynamics theory, jet penetration is inversely proportional to the square root of the ratio of density of the target (22) and the jet.

$$P = L (\rho_j / \rho_t)^{1/2}$$

P = total penetration

L = length of the jet

ρ_j = jet density

ρ_t = target density

This equation does not appear to be valid for non-ductile targets such as rock. In 1962, Thompson (24) showed that penetration was proportional to the compressive strength of rock. Although the densities of rock used were far less than that of steel "penetration in rock having high compressive strength has been observed as similar to that obtained in steel". Thompson's work can be summarized by Figs. 11 and 12. Testing of rocks within the range 1,000-1,500 psi compressive strength was reported to show that valid estimates of penetration can be based on compressive strength.

Because the emphasis in perforating has been on maximum depth of penetration, no theory is available to predict hole size in a target. All comparative test procedures have incorporated data on the entrance hole size in addition to the depth of penetration.

Early attempts to compare the penetration of different perforators used cement targets. A cement slurry is poured into a small-size casing. One end is closed with 3/8-in. mild steel plate welded to the pipe. Many serious attempts to obtain consistent cement targets were tried; Dresser Atlas (21), among others, mixed the slurry under vacuum to achieve consistency by eliminating air bubbles.

The concrete test target is one of the two methods described by API RP 43'rd edition to evaluate well perforators. The cement mix is rigidly specified (25):

- 1 part or 94 lb. (1 sack) of API class A cement
- 2 parts or 188 lb. of washed and graded dry sand
- .45 part or 42.3 lb. (5.1 gallons) of potable water.

Sieve analysis requirement is reported on Table 1. Casing or tubing is to be centered in the target form, and the slurry poured around it, Fig. 13. The concrete target is to be cured for 28 days at temperature greater than 40°F and under at least 3-in. of water. Finally, the tensile strength shall exceed 400 psi.

Summary of Previous Work and Its Relation to this Study

Becher (26) summarized the work done on emulsions by the following:

"It is unfortunate fact that there exists no single coherent theory of emulsion formation and stability. By and large the various workers in the field, even in theoretical discussions, have limited themselves to specialized systems; and what was found to be true for certain systems under certain conditions is not necessarily applicable to other systems... The prediction of emulsion behaviour is still largely a matter of art rather than science."

Despite this fact, the previous review can be summarized:

1. The contrast in viscosity between cement slurry and air enhances stability but makes the foam hard to form.
2. Lowering the surface tension by adding a surface active agent helps to minimize the thermodynamic instability of the system and accelerate the foaming process.
3. The smaller the bubbles and the narrower the bubble size distribution, the more stable is the foam.
4. Extreme rates of shear might be necessary to achieve a small bubble size and uniform size distribution.

5. Since the slurry is actually a suspension of fine solid particles, foam cement can be stable; moreover, the presence of high valence metals (aluminum, for example), will help long time stability.

Concerning Jet Perforation:

1. Most jet perforation tests are carried out to evaluate perforators; therefore, the tendency is to use high compressive strength targets.

2. There is no significant increase in compressive strength of foam cements beyond three days curing time.

3. No data is reported for jet perforating targets having compressive strengths less than 1,000 psi.

Definitions

In this study, quality is defined as the ratio of the volume of the free gas contained in a slurry to the total volume of the slurry. Porosity is assumed equal to quality. Quality is determined by the following relation:

$$\text{Quality} = \frac{\text{Density of neat slurry} - \text{Density of foamed slurry}}{\text{Density of neat slurry}}$$

Foam cement was called stable when a three-foot vertical sample set before any drastic change of density occurred between the top and the bottom of the column.

A slurry was called homogeneous when small samples obtained from a given batch did not show any consistent changes in density.

EXPERIMENTAL PROCEDURE

Initially, a procedure for mixing a foam cement slurry was investigated in which nitrogen was injected into the cement slurry through a nozzle, Fig. 14. This setup produced foam, but it was not stable, Fig. 15.

Paint Shaker

The large slurry volume required for each sample precludes the use of Waring blender for foaming the slurry. An alternate method was found which allowed the mixing of a large volume of foam cement: A paint shaker, Fig. 16.

The agitation of a paint shaker consists of a cyclic combination of two movements: a translation along the X axis and a rotation in the YZ plane. The mechanism yielding to such a movement is schematically represented in Figs. 17a and 17b.

Let "A" be a point on the shaft located by its abscissa x on the X axis and angle α from the vertical, in the YZ plane. The movement of "A" during one revolution is described by the following:

1-2. "A" moves from $x = -x_0$ to $x = 0$ while rotating from $\alpha = 0$ to $\alpha = +\theta$.

2-3. "A" continues its linear movements from $x = 0$ to $x = +x_0$ on the X axis, but reverses the rotation from $\alpha = +\theta$ to $\alpha = 0$.

3-4. "A" reverses its motion from $x = +x_0$ to $x = 0$, but continues the same direction of rotation from $\alpha = 0$ to $\alpha = -\theta$.

4-1. "A" moves to its original position from $x = 0$ to $x = -x_0$ and from $\alpha = -\theta$ to $\alpha = 0$.

The cycle described above is completed in .092 sec. (750 rpm). The change in the direction of movement every .023 sec. is believed to be the reason for the "high shear" resulting in small and uniform bubble size observed for each batch.

Physical or mathematical study of the effect of the paint shaker movement on the cement slurry is a complex hydrodynamic problem and was considered beyond the scope of this study.

A container holder was attached to the shaft of the paint shaker and two-gallon air-tight containers were used. One advantage offered by this "closed container" method of mixing was its ability to generate the desired quality slurry. The controlled sample was achieved by controlling the cement slurry volume to be foamed.

$$\text{Quality} = \frac{\text{Air Volume}}{\text{Total Volume}} = \frac{\text{Container Vol.} - \text{Slurry Vol.}}{\text{Container Volume}}$$

The equation above does not take into account the volume of air introduced into the cement slurry during the mixing prior to the shaking action.

Originally, two paint shakers were used, but it was found that they did not have the same type of agitation.

A batch was divided in two: batch #1 and batch #2. Batch #1 was shaken in paint shaker "A" and batch #2 in paint shaker "B". After thirty minutes shaking time, batch #1 container was full of foam cement, yielding the desired quality; while batch #2 was not. Batch #2 was then shaken in paint shaker "A". Fifteen minutes was enough to fill up the container and yield the desired quality. Paint shaker "B" was not used after the initial experiment.

Preliminary Tests

Some preliminary tests before the final sample preparation procedure need to be mentioned.

First, the following mixing procedure was tried: dry cement and water were mixed. Surfactant was then added to the slurry. The batch was shaken for thirty minutes. The result was a definite non-homogeneous foam cement. The change of quality with sample sequence is shown on Fig. 18.

A batch mixed according to the procedure above was injected into a three-foot long, one-inch inside diameter, plexiglass tube, Fig. 19. The low density foam, although displaced last, broke through the high density slurry displaced first and resulted in a typical unstable foam cement. Fig. 20 shows the distribution of quality along the sample after setting.

An ultimate case was obtained when unmixed water and cement were accidentally trapped in the injection line. After foam was injected in the plexiglass tube and the system set, there was a definite

separation between foam, water, and cement, Fig. 21.

When the surfactant was diluted in water before dry cement was added to the solution, the result was a very homogeneous foam, Fig. 18. A similar slurry was injected in a vertical plexiglass tube. No noticeable segregation between top and bottom was noted, Fig. 20.

Shaking time significantly influenced the size of the air bubbles in the foam cement slurry. The longer the shaking time, the smaller the bubbles. Time, however, had to be restricted to thirty minutes to allow for slurry handling without excess thickening or premature setting.

The minimum amount of surfactant necessary to produce any given quality was experimentally established, Fig. 22. A slurry with known surfactant concentration was shaken for fifteen minutes. If the container was not full after this shaking time, a higher concentration was needed. If the container was full, a lower concentration was tried.

Sample Preparation

In order to minimize any effects the surfactant might have on the strength of the foamed cement and, at the same time, ensure proper foaming of the cement slurry, surface agent Adofoam was diluted in water in a proportion slightly above the concentration requirements previously mentioned. Dry cement (Class G) was slowly added to the solution in a two-gallon dough mixer, rotating at 60 rpm. After five minutes initial mixing time, the slurry was poured into a two-gallon

plastic container. The container was sealed, placed in the holder of the paint shaker and shaken for thirty minutes. This procedure was used for all samples except for neat cement, of course, and samples with qualities less than twenty percent. At such qualities, the paint shaker load was exceeded (24 lb.); dividing the batch in two parts became necessary. Each part was shaken for fifteen minutes; the appropriate surfactant concentration was determined from Fig. 22.

The foam slurry obtained was poured into a 3-ft., 4 1/2-in., 11.6 lb./ft. casing section to which a bottom plate had been previously welded. Four small samples were collected while the pipe was filled and their densities immediately measured with a mud balance. This random sampling of the batch helped check the homogeneity of the foamed slurry, Tables 6 through 17.

A total of twelve samples were produced within forty-eight hours; they covered a range of qualities from zero to fifty percent. For every quality, two slurry compositions were used: one with thirty percent silica flour, the other without.

Cement cured in the pipes for ten days at room temperature and atmospheric pressure before a 1/2-in. top plate was welded to the pipe, flush against the cement surface.

The samples were shipped to the Dresser Atlas Laboratories in Houston, Texas, for perforation test.

Perforation Test

The charge used for the perforation was a 4-in. Dresser Atlas Jumbo Jet. A "premium charge ... selected for its consistency". All samples were shot in air according to the set up shown in Fig. 23.

Scaling the jet perforator down to prevent shooting completely through the samples became necessary. This was accomplished through the use of 1-in. mild steel plates between the charge and the target. A single 1-in. plate was used on all tests except for samples #3, #5, #6, and #7 where two plates were used.

The samples were perforated in a seven-day period. To prevent loss of any eventual materials in the perforation during shipment, the holes on the top plates were plugged with corks. The total curing time before perforation averaged forty days.

When the samples arrived, the perforations were filled with wax in order to penetrate any cracks caused by the jet perforator.

Every sample was cut in thirds. The top and bottom plates were removed and a code name was assigned to every face of every section. One by one, the sections were run through a milling machine, and a slot 1/4-in. wide was cut along the metal sleeve. When the metal jacket was totally open, it caused the slot to widen to 3/8-in.

RESULTS AND DISCUSSION

The paint shaker permitted the obtention of large batches of homogeneous foam cement, with qualities very close to those intended. The paint shaker, however, did not guarantee the homogeneity of the slurry, Fig. 18. The procedure used to mix the slurry was the principal factor affecting slurry homogeneity.

Mixing

When a batch was mixed according to the first procedure discussed in Chapter II, the surfactant, although highly soluble, did not associate with every molecule of water in the slurry: The hydration of cement particles begins at the instant dry cement and water are in contact. After a few minutes (27), most water molecules have already reacted with the Tricalcium Alluminate, and part of the Dicalcium and Tricalcium Silicate present in Class G cement. When surfactant is added to the cement slurry already under setting and hardening reactions, little water is available to mix with the surfactant. The foaming agent is unevenly distributed in the water body causing very high concentrations in some parts of the slurry.

When surfactant is diluted in the water to be mixed with dry cement, every cement particle "sees" the same amount of surface active

agent. The ability to trap an air bubble is the same for all parts of the slurry.

Once the homogeneity was realized, the stability was practically insured. Beside homogeneity, the success in obtaining three-foot long columns of stable foam cement must be attributed to the microscopic bubble size produced by the paint shaker. Every batch collected looked like "shaving cream". To achieve such a small size, the paint shaker must have developed a very high shear action throughout the slurry, (Appendix A). Examining the bubble size on set samples, one notices that coalescence had taken place. This, however, seems to be a localized phenomenon since the analyzed columns satisfied the criterion for stability defined earlier in the text. Two actions take place in the setting sample: coalescence of the air bubbles and hardening of the cement. Because the bubbles in the foamed slurry are extremely small, it takes longer for a number of bubbles to form a single, large bubble than for the cement to set or at least to thicken. Bubbles become larger in the set cement as quality increased; this can be explained by the tighter packing of the bubbles in higher quality samples. If the rate of coalescence were determined, one might predict the bubble size and possibly the bubble size distribution in set foam cements.

Adhesion to Casing

The foam cement samples with qualities less than twenty percent slid easily from the casing after cutting, leaving small amounts of powdered cement on the inside wall of the pipe.

For the thirty and forty percent quality samples, it was necessary to force the sample out of its sleeve using a wooden hammer.

With the fifty percent quality samples, it was impossible to slide the samples out of the cut casing. One sample was actually ruined when the wooden hammer was used. A second slot, diametrically opposed to the first one, was cut through the metal of the other samples. Even then, the metal shell did not separate from the core until force was used. More than a 1/4-in. thick layer of foam cement adhered to most of the inside wall of the casing, Fig. 24.

The impossibility of sliding high quality foam cement through the pipe suggests an unexpected shear bonding strength. An accepted relationship between compressive strength and shear bonding strength (28), is shown on Fig. 25. In view of the above remarks, such a relationship, valid for neat cements, is probably not applicable to foam cements.

Perforation

Underneath the top plate, the cement surface was damaged for all samples. Most cracks and fractures were essentially located at the outer radius of the surface (chipped edges). Such damage probably occurred while removing the top steel plate, because, except for sample #10, there is no wax present within the cement body beyond the perforation wall. The extent of damage is particularly noticeable for the fifty percent quality samples, Figs. 26 and 27.

Some fractures extending radially along the perforation wall are noticed. Section faces were compared before the sleeve was removed and after removal. The rupture present in the core when the jacket was off was not visible before removal. The fracture was caused by the release of the confining pressure of the casing.

The samples were longitudinally cut using a core cutter. Fig. 28 shows the difference in hole diameter for two samples of comparable qualities. One of them was shot through a single 1-in. mild steel plate; the other through two 1-in. plates.

Because of this difference in shooting conditions, the perforation diameter was correlated to quality using two sets of data, Fig. 29. The hole size increases with quality for both sets of data. Fig. 29 also shows that addition of silica flour has no significant effect on the perforation diameter.

Attempts to correlate total penetration with quality was unsuccessful. Despite the efforts to scale down the jet perforator, the perforation totally penetrated five out of the twelve samples. In sample #1, the perforation penetrated all the way through the bottom plate, Fig. 30. When these five data points are not considered, there is very little to correlate. Only samples #9, #10, #11 and #12 were shot under identical conditions. The necessary correction suggested by W.A. McPhee (see Appendix B) did not yield the desired results, Fig. 31.

When wax was removed from the perforation, very few cement crumbs were present. The largest fragments encountered were less than .1-in. in size. Powder-like cement particles coated the filling wax, as well

as the perforation wall for samples with qualities greater than twenty percent. For lower quality samples, the perforation was relatively dust-free.

Along the wall of the perforation, a very interesting feature of foam cement is observed. Fig. 32 is a longitudinal cross section of sample #11 (neat cement). Fig. 33a is a longitudinal cross section of sample #1, fifty percent quality. Both samples were shot under the same conditions. Before the picture on Fig. 32 was taken, the surface was wet with water. A network of fine fractures throughout the surface is visible. On Fig. 33 there is a different situation. The light colored strips on both sides of the perforation represent the compacted zone. A magnified view of Fig. 33a is shown on Fig. 33b (actual size). The compacted zone extends radially about 1/4-in. from the perforation wall. Hardly any pore space is observed in this zone, but no noticeable disturbance in the pore structure or the cement matrix exists beyond it. This striking difference between neat cement and foam cement is due to the brittle state of neat versus the almost "plastic" behaviour of foam cement. When neat cement is perforated, it is subject to stresses along the perforation axis. Because of its brittle state, very little "plastic" deformation takes place. A stress-strain curve, Fig. 34a, describes the brittle state of neat cement. At point C, the specimen breaks. The curve is initially linear and shows little or no curvature as point C is approached.

Foam cement, on the other hand (especially high quality cement), exhibits a more "plastic" behaviour when under stress, Fig. 34b. The surface upon which stress is applied caves in first and the matrix is crushed into the surrounding pores. The rise in region AB beyond the yield stress is because of strain hardening (denser structure at the stressed surface). This may be regarded as an increase in the yield stress of foam cement caused by the deformation.

Copper and steel particles were embedded in fractures along the perforation wall for neat and low quality cement. For higher quality foam cement, metal debris of the shaped charge and top plates were found filling up the far end of the perforation. This is another difference in the behaviour of foam cement when jet perforated. In the case of neat or low quality cement, when the charge is detonated, the flow of the liquified copper liner and steel plates is diffused into the open fractures initiated by the jet impact. The total mass of the after jet is distributed into the fractured matrix. Small amount of metal debris remains as a slug embedded in the bottom of the perforation. This results in the seemingly carrot-free perforation.

In the case of higher quality foam cement, the high velocity jet crushes the matrix radially creating a denser layer of material around the hole. The slug penetrating the hole with lower velocity cannot diffuse radially. Its path of least resistance will be along the perforation; its movement is finally stopped at the far end of the perforation.

This feature might constitute some handicap for foam cement use for completion, since the entire slug will be embedded in the producing formation. This handicap is, however, easily compensated by the fact that with foam cement in the annulus, the jet is subject to less resistance; therefore, the depth of penetration is much greater than with neat cement.

For qualities below forty percent, foam cement shows no damage susceptible to deter its use in well completions. The perforated hole is large, smooth and cylindrical; produced fluids will meet no obstruction in flowing through jet-perforated foam cement into the production string.

Conclusions

The following conclusions are reasonably supported by this study:

1. Perforation diameter increases with quality.
2. Penetration of jet increases with quality.
3. Decrease in perforation diameter with depth is uniform.
4. For qualities less than forty percent, foam cement can be jet-perforated without excessive fracturing around the perforation.
5. A zone of altered foam cement was found adjacent to the perforation and extended radially from it. The zone appeared to be more dense than the unaltered matrix.
6. Foam cement adheres to casing.
7. Stable foam slurries may be created with an agitation developed by a paint shaker.

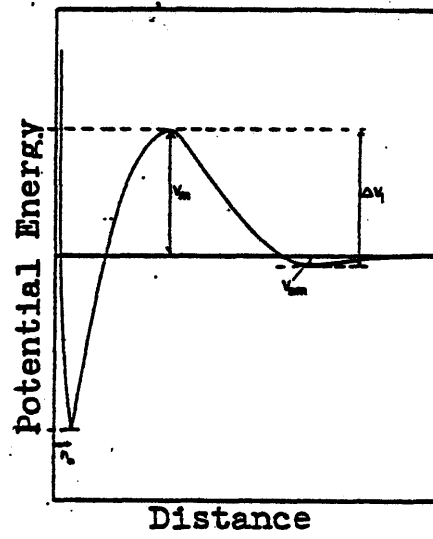


Fig. 1. Schematic Form of the Curve of Total Potential Energy, after Ottewill (11).

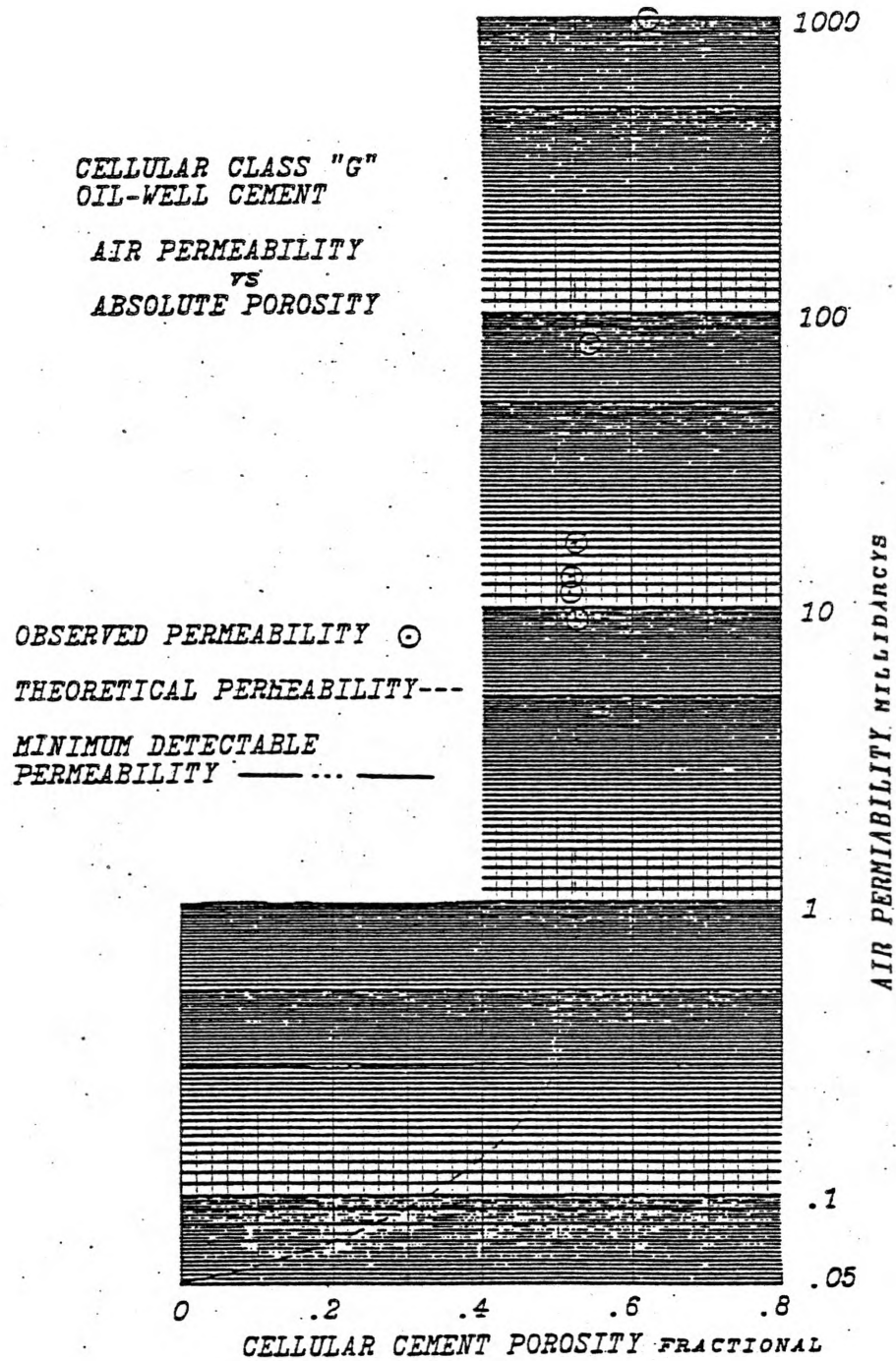


Fig. 2. Permeability of Foam Cement, after Aldrich (17).

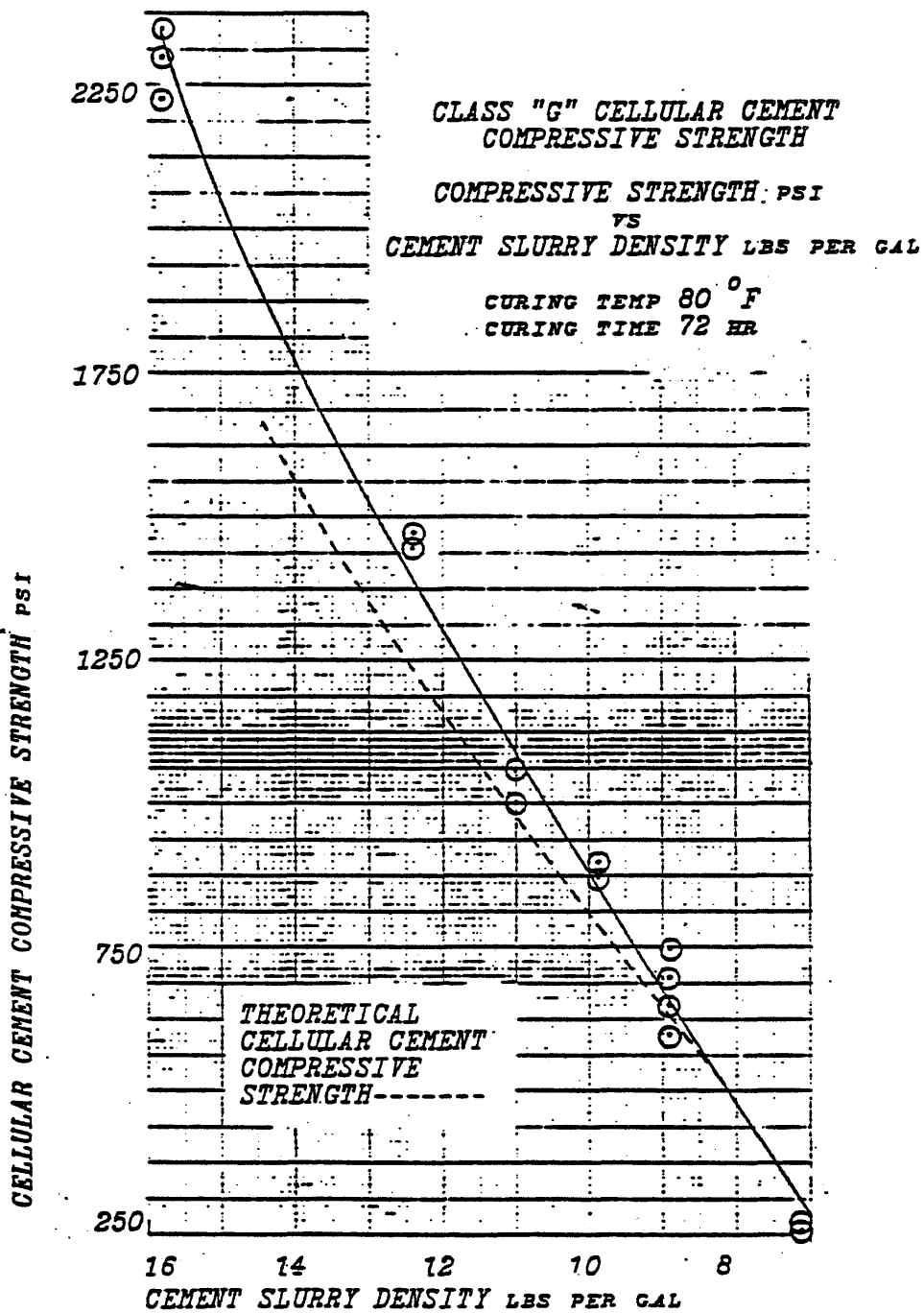


Fig. 3. Compressive Strength of Foam Cement, after Aldrich (17).

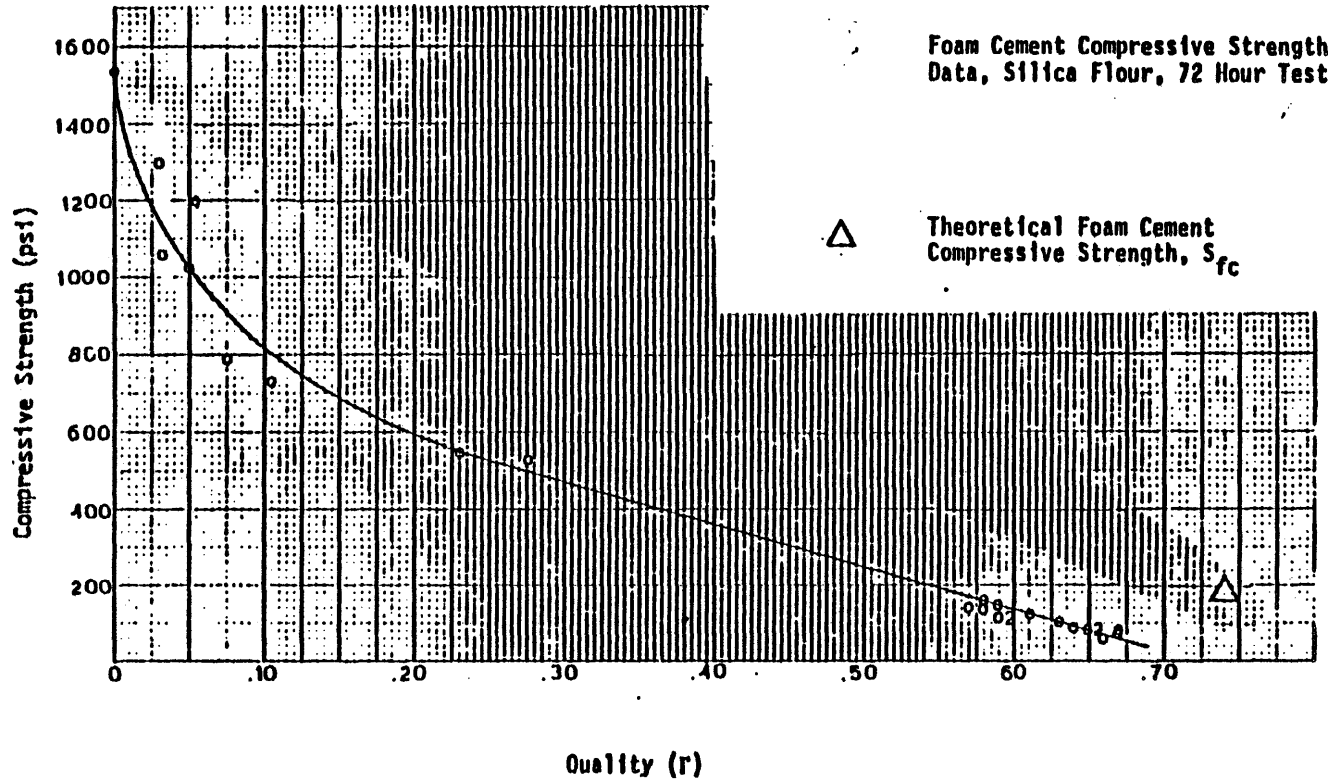


Fig. 4. Compressive Strength of Foam Cement-Silica Flour, after Slattery (18).

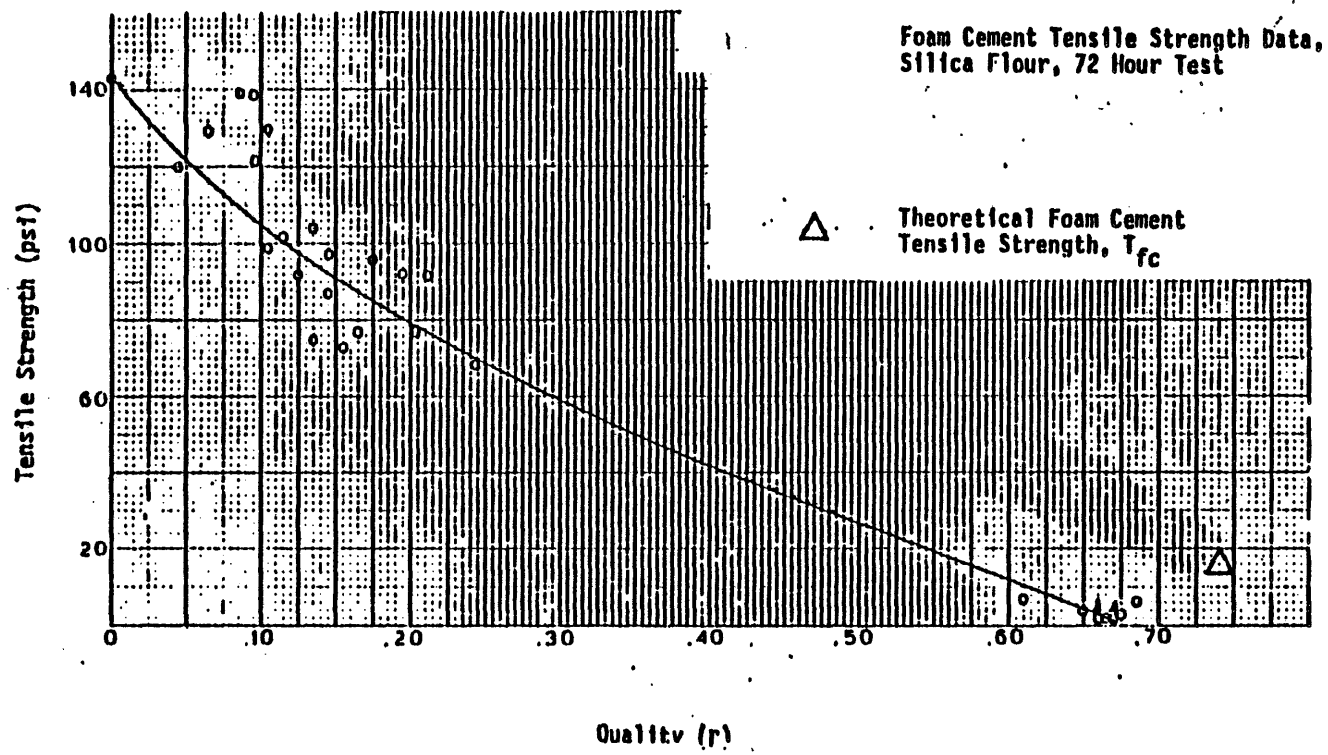


Fig. 5. Tensile Strength of Foam Cement-Silica Flour, after Slattery (18).

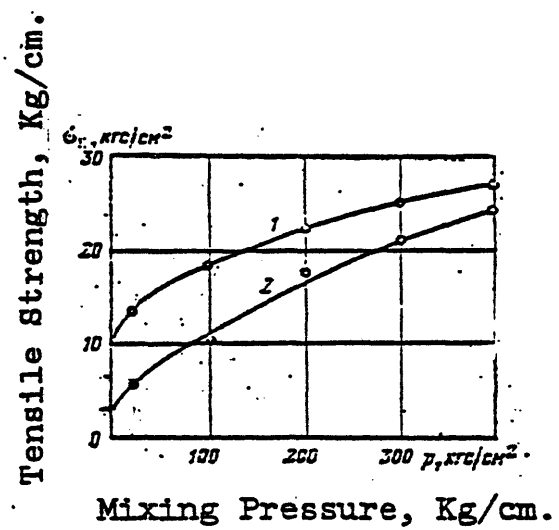


Fig. 6. Tensile Strength versus Mixing Pressure, after Detkov and Sabrizyanov (19).

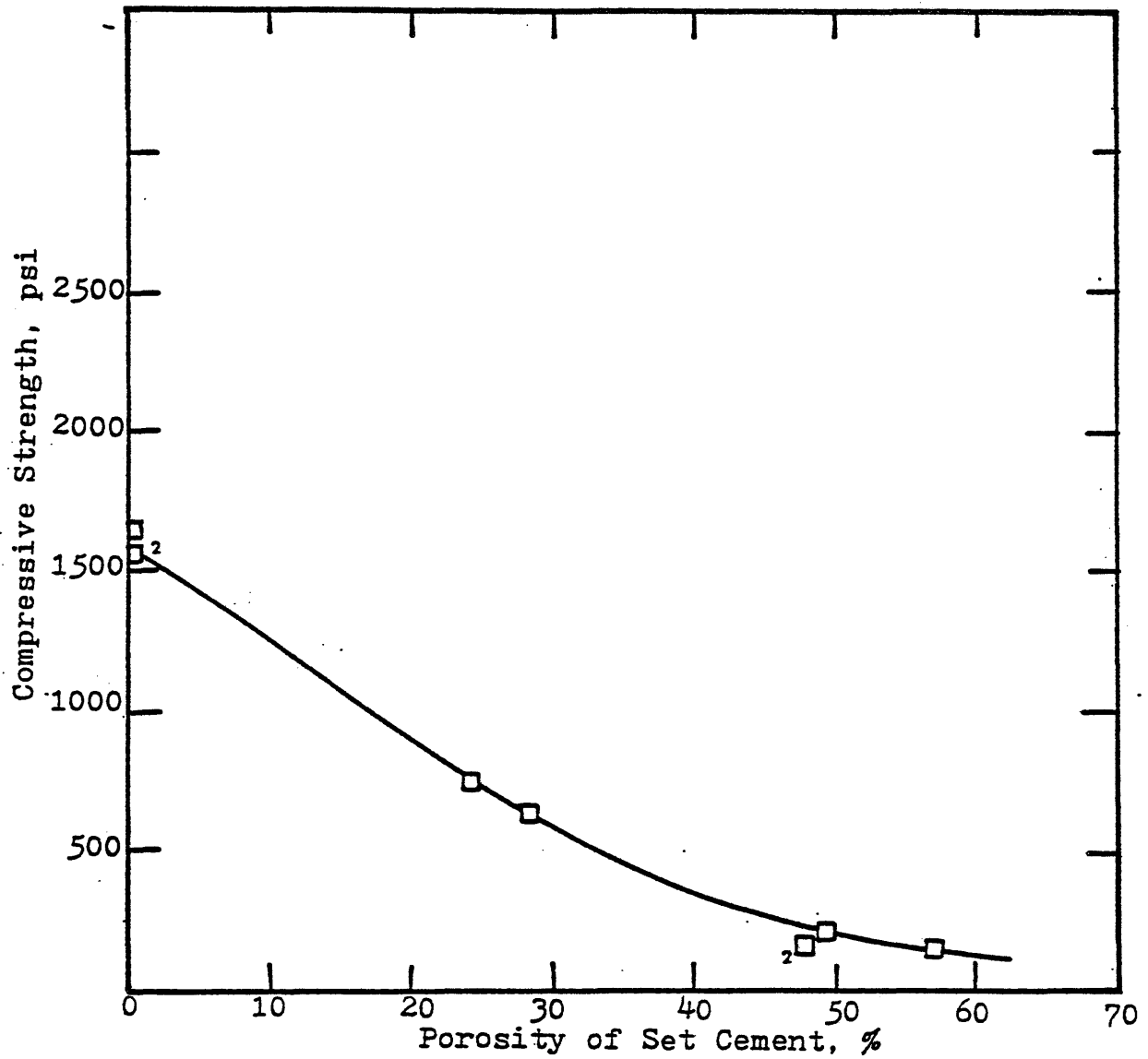


Fig. 7. Foam Cement Compressive Strength Versus Porosity of Set Cement, 28 days, 140°F, after Pakbaz (20).

am

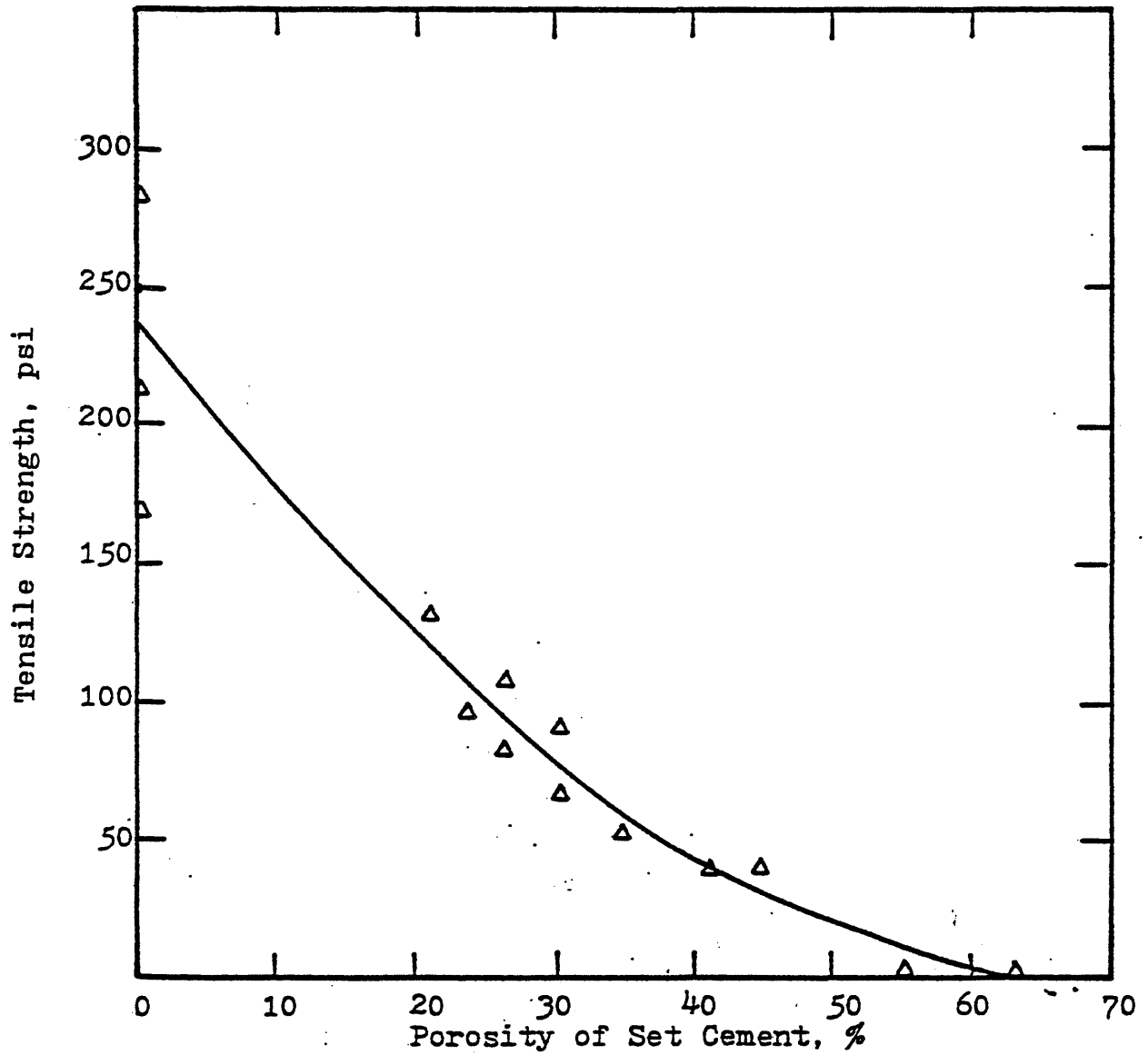
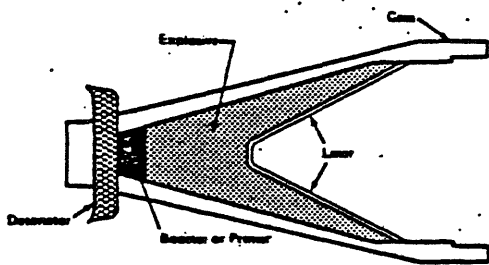
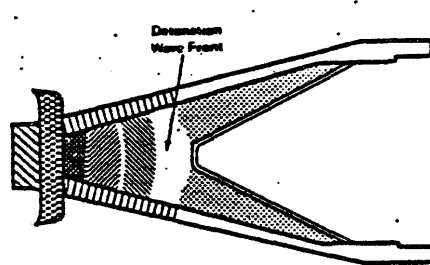


Fig. 8. Foam Cement Tensile Strength Versus Porosity of Set Cement, 28 Days, 140°F, after Pakbaz (20).



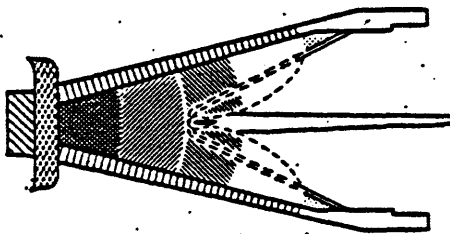
(a)

Major Components of Shaped Charge Perforator



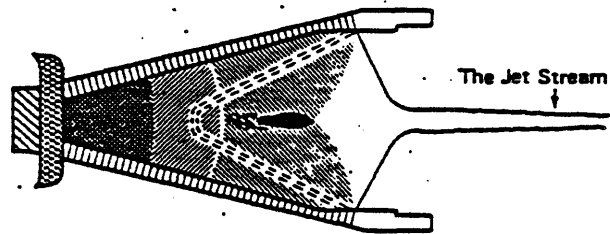
(b)

Detonation travels down the charge and strikes the Apex of the Cone



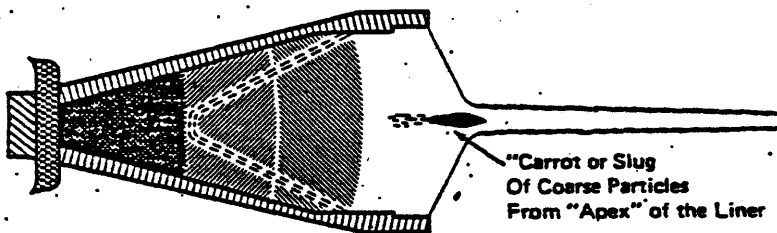
(c)

Wavefront collapses Liner. The Liner's inner surface disintegrates to form part of the Jet Stream.



(d)

Advancing wavefront forms the Jet Stream. The outer surface of the Liner forms a Slug or Carrot which follows the Jet Stream



(e)

The fully developed Jet Stream penetrates a target, the Carrot follows with no contribution.

"Carrot or Slug Of Coarse Particles From "Apex" of the Liner

Fig. 9. Detonation Stages of a Typical Shaped Charge, after "Perforation Technology" (21).

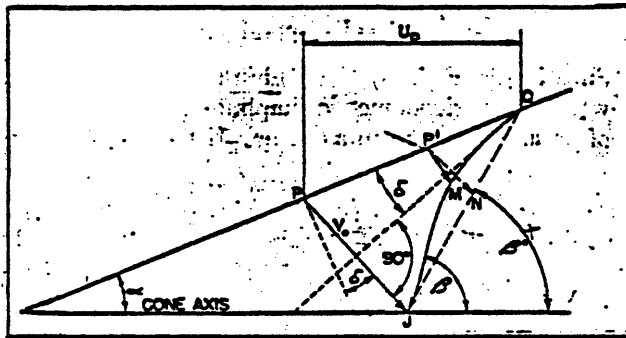


Fig. 10. Cross Section Showing the Collapse Process in a Conical Liner, after Pugh et al. (23).

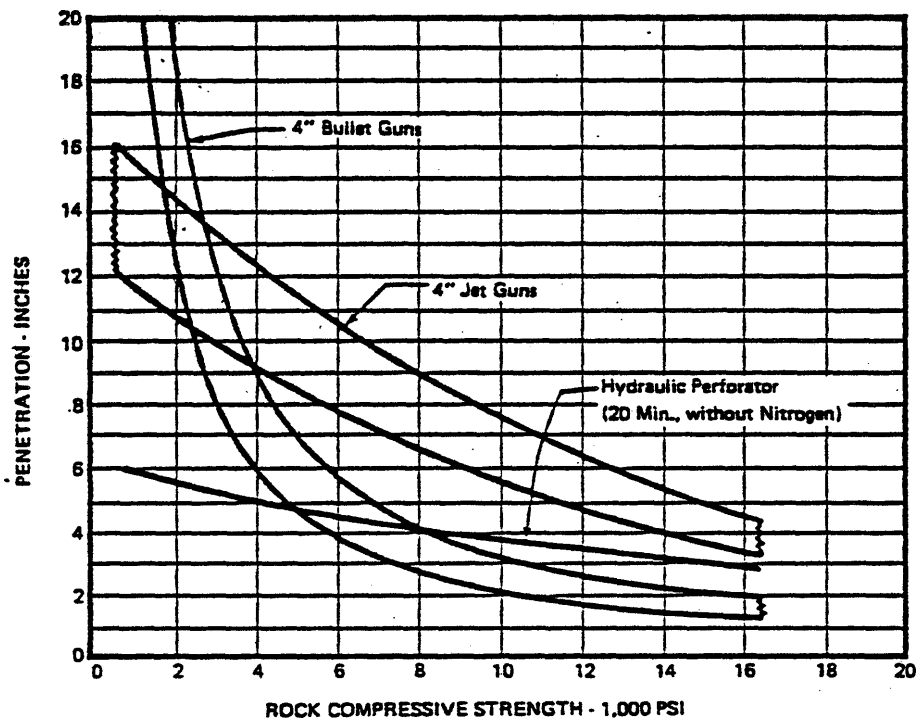


Fig. 11. Bullet, Jet and Hydraulic Perforator Performance, after Thompson (24).

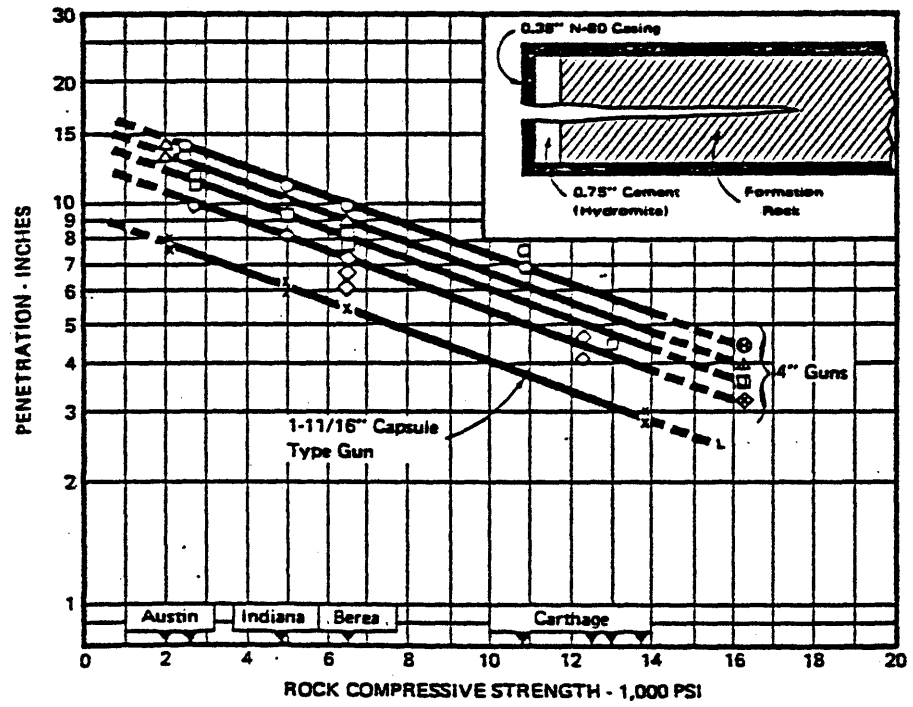


Fig. 12. Jet Penetration vs. Formation Strength, after Thompson (24).

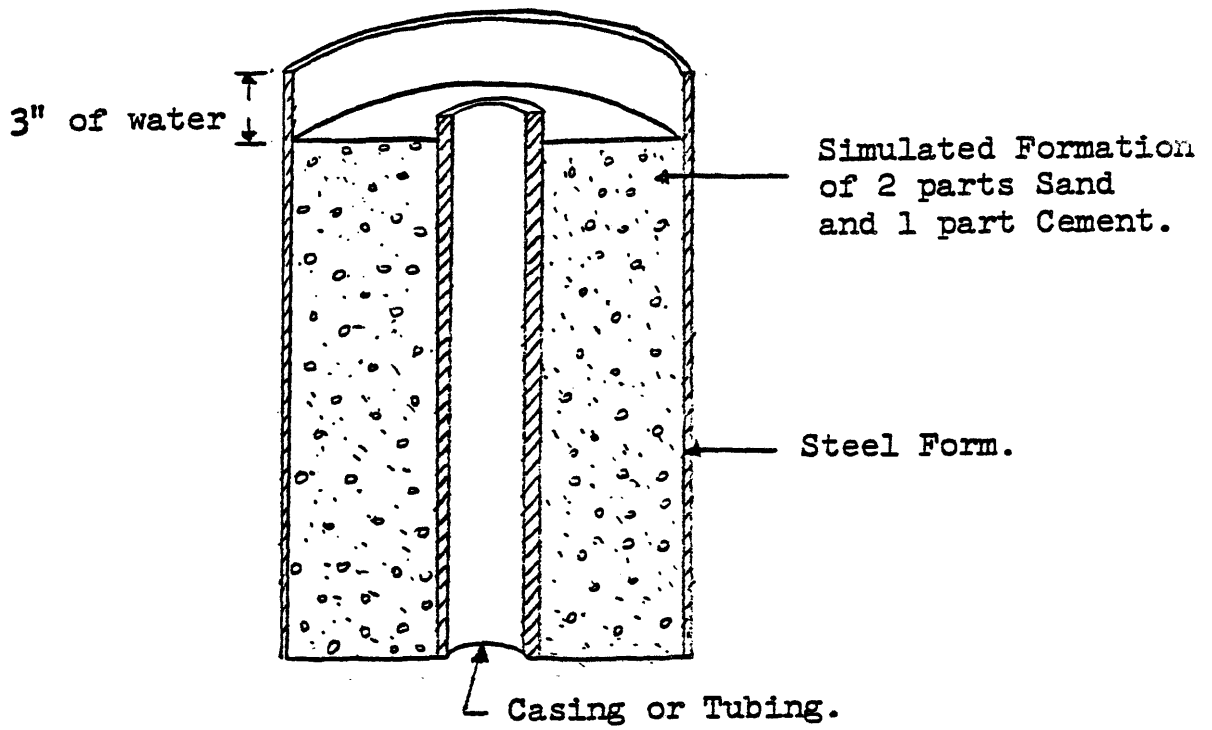


Fig. 13. Concrete Test Target, (25).

42

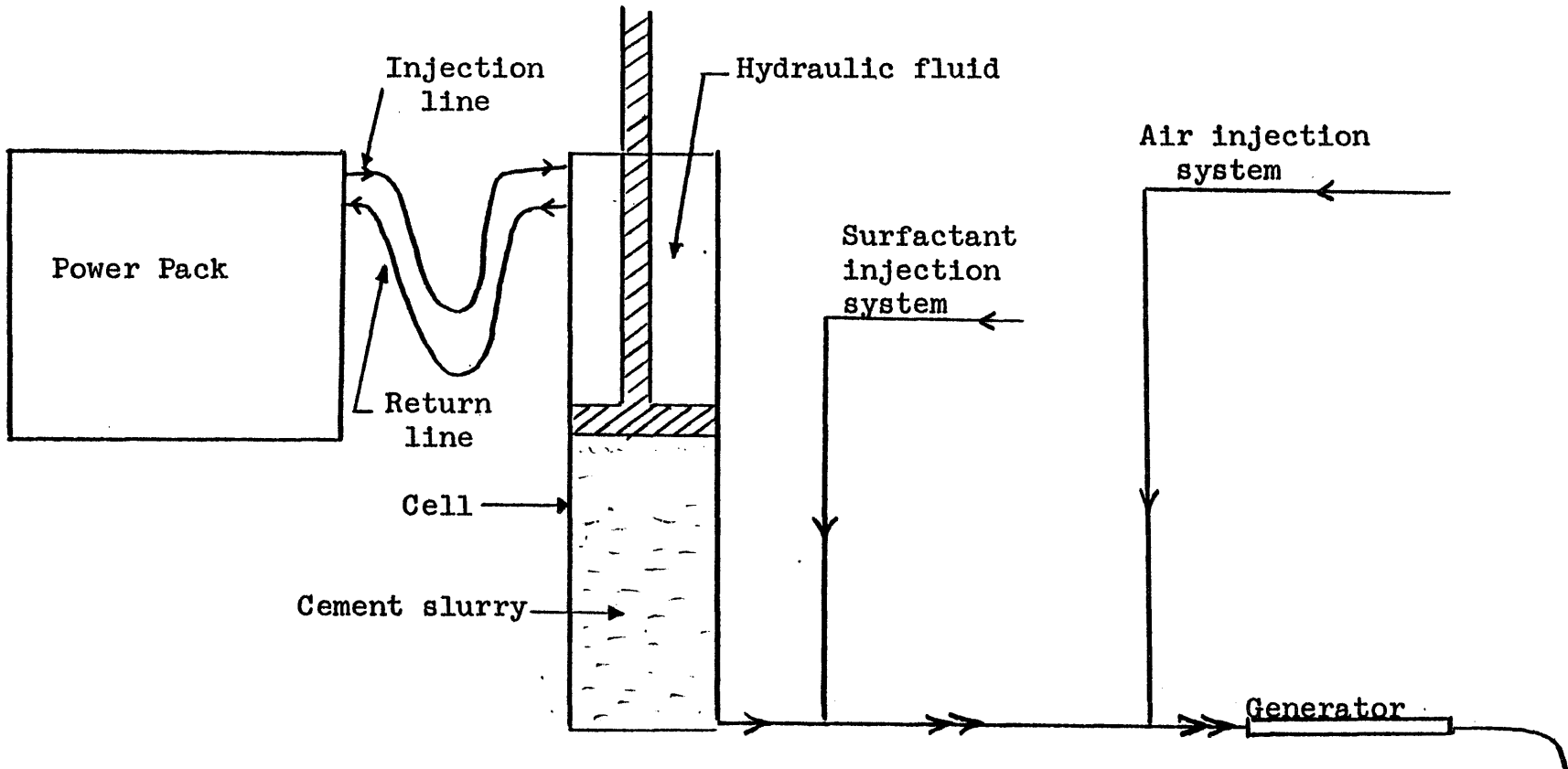


Fig. 14. Foam Cement Injection System.

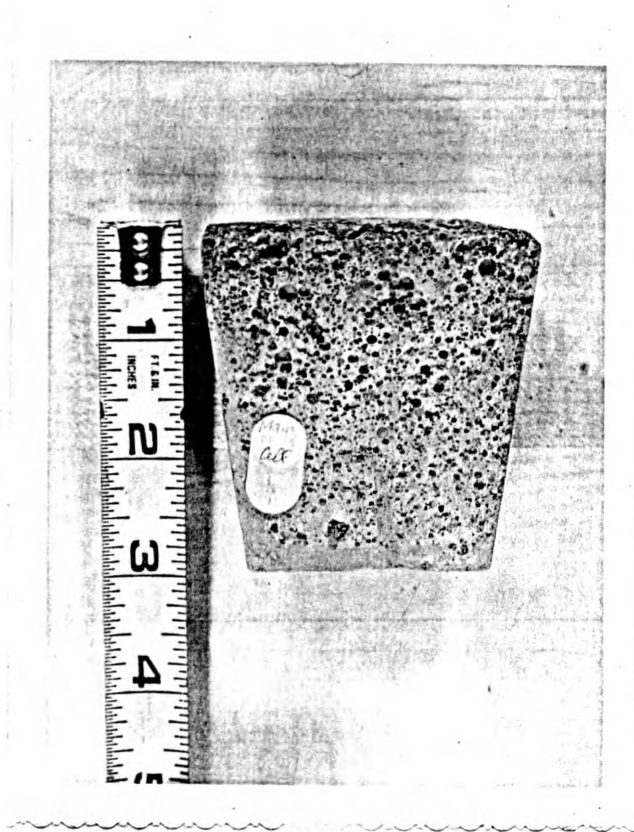


Fig. 15. Segregation along a 3 in. sample.

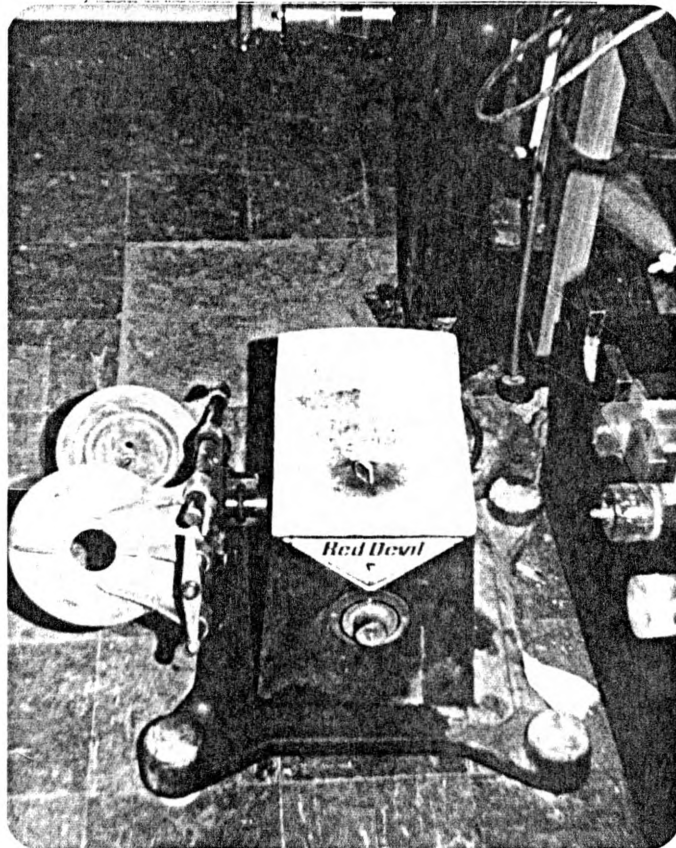


Fig. 16. A Paint Shaker.

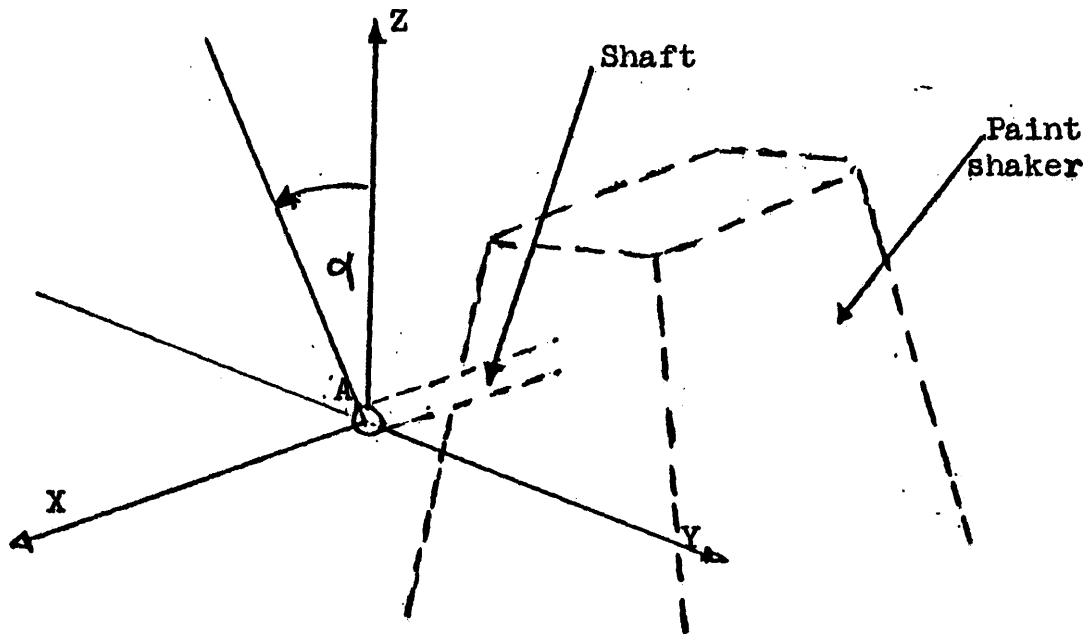


Fig. 17a. Paint Shaker (Schematic).

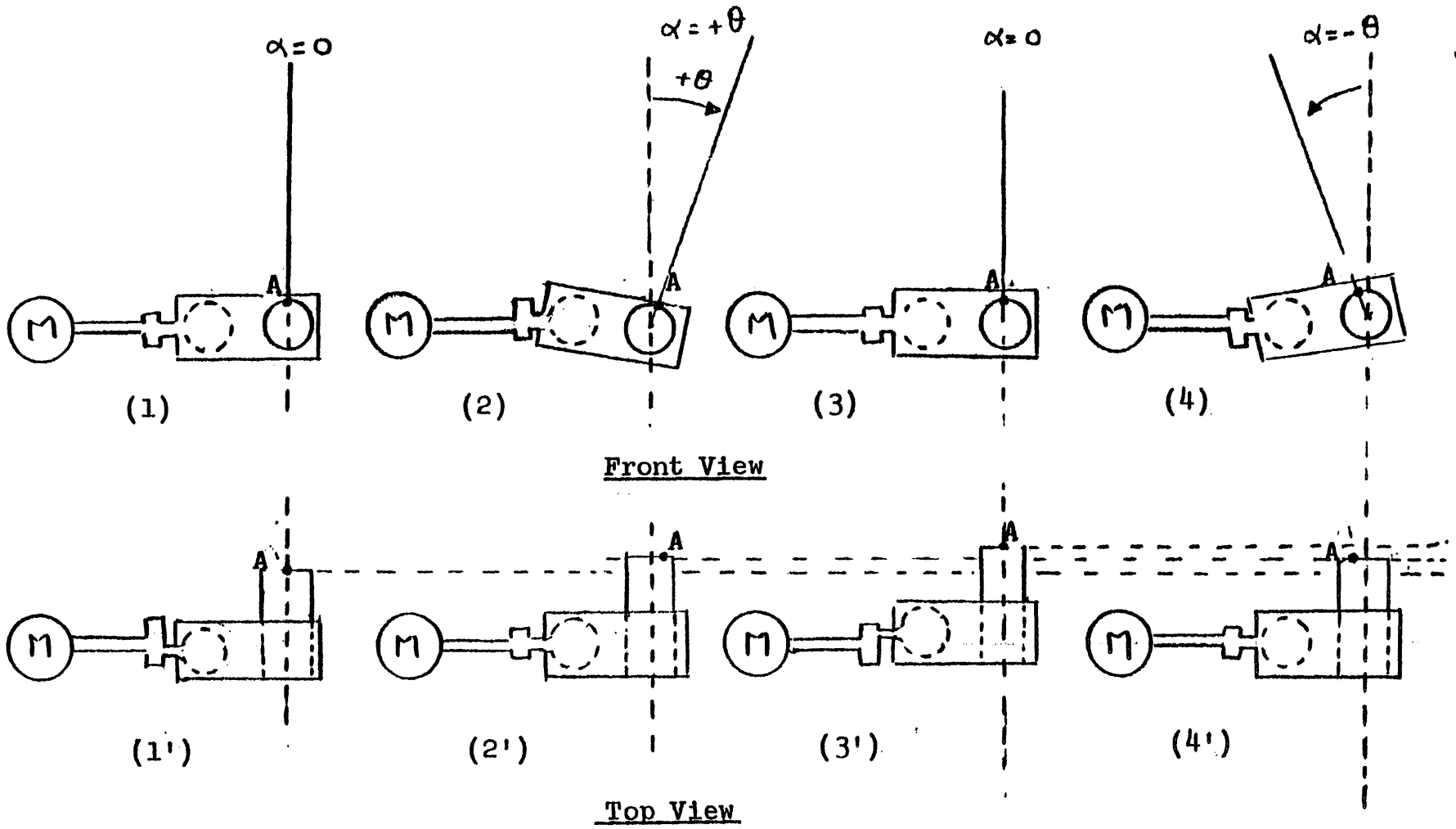


Fig. 17 b. Schematic Representation of a Paint Shaker's Movement.

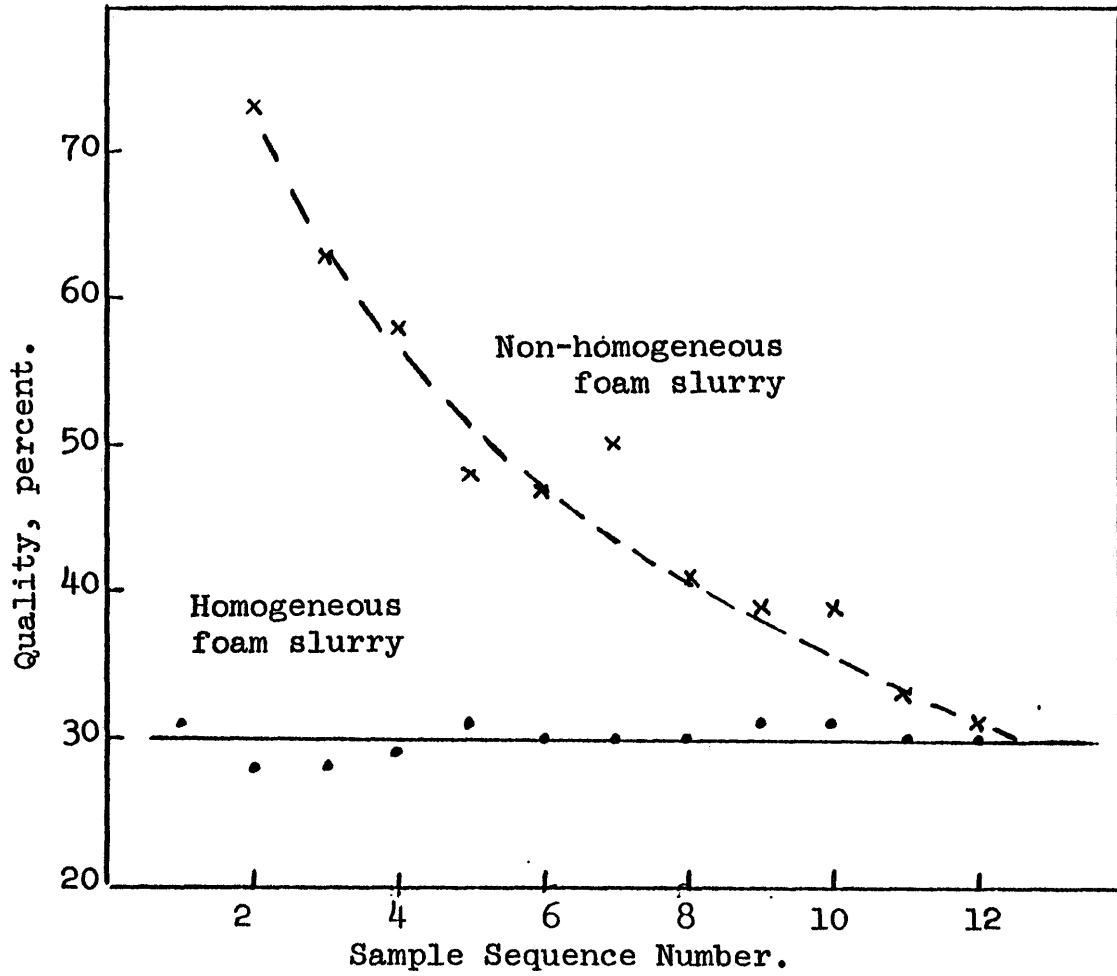


Fig. 18. Typical Batch Homogeneity Analysis.

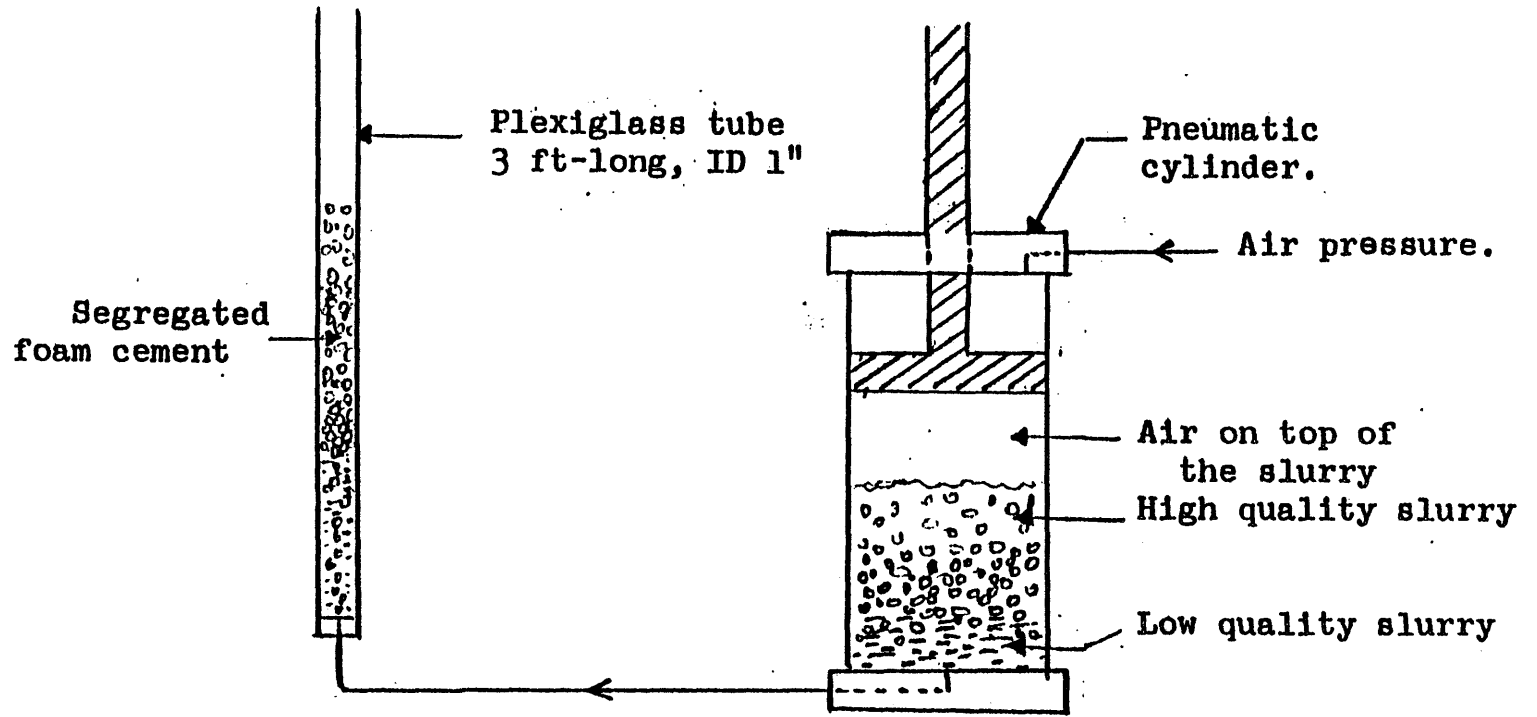


Fig. 19. Injection System into a Plexiglass Tube.

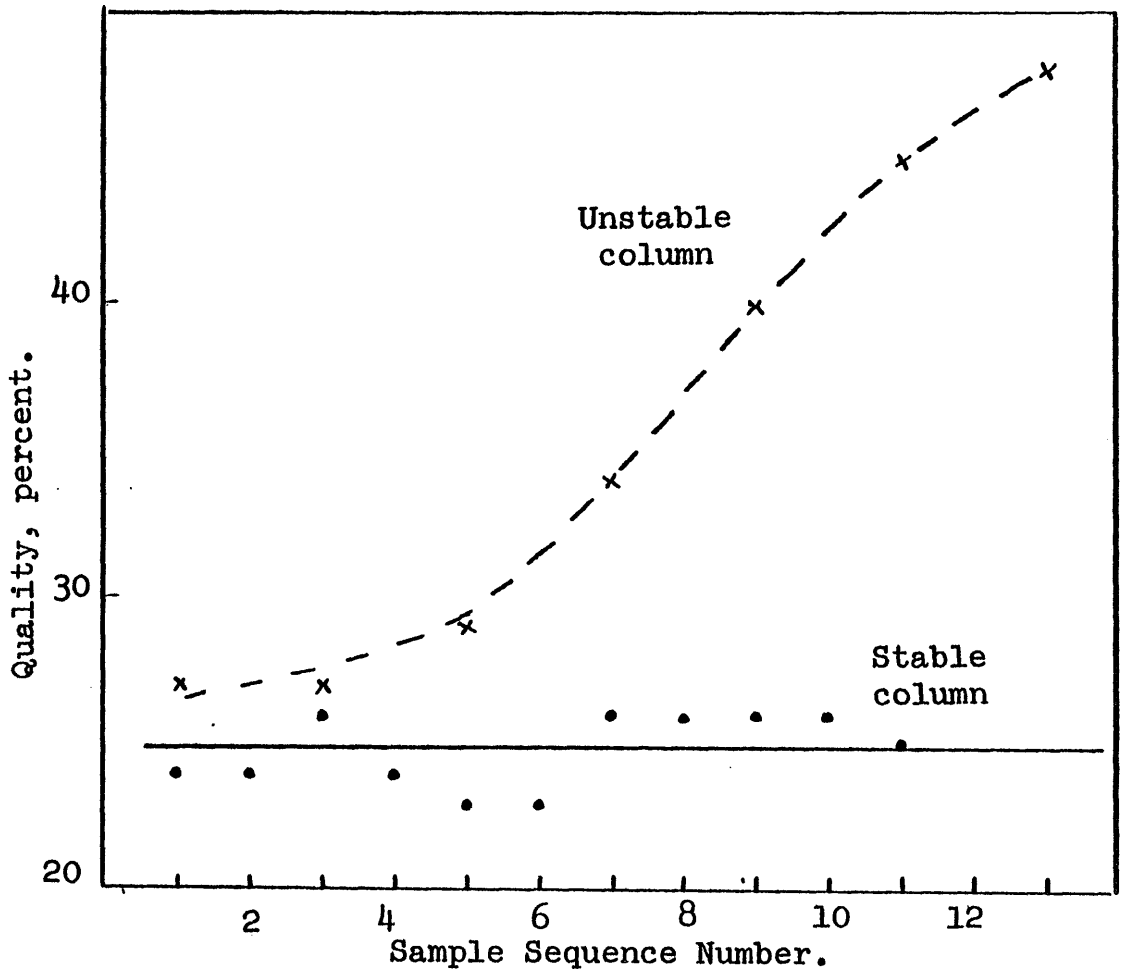
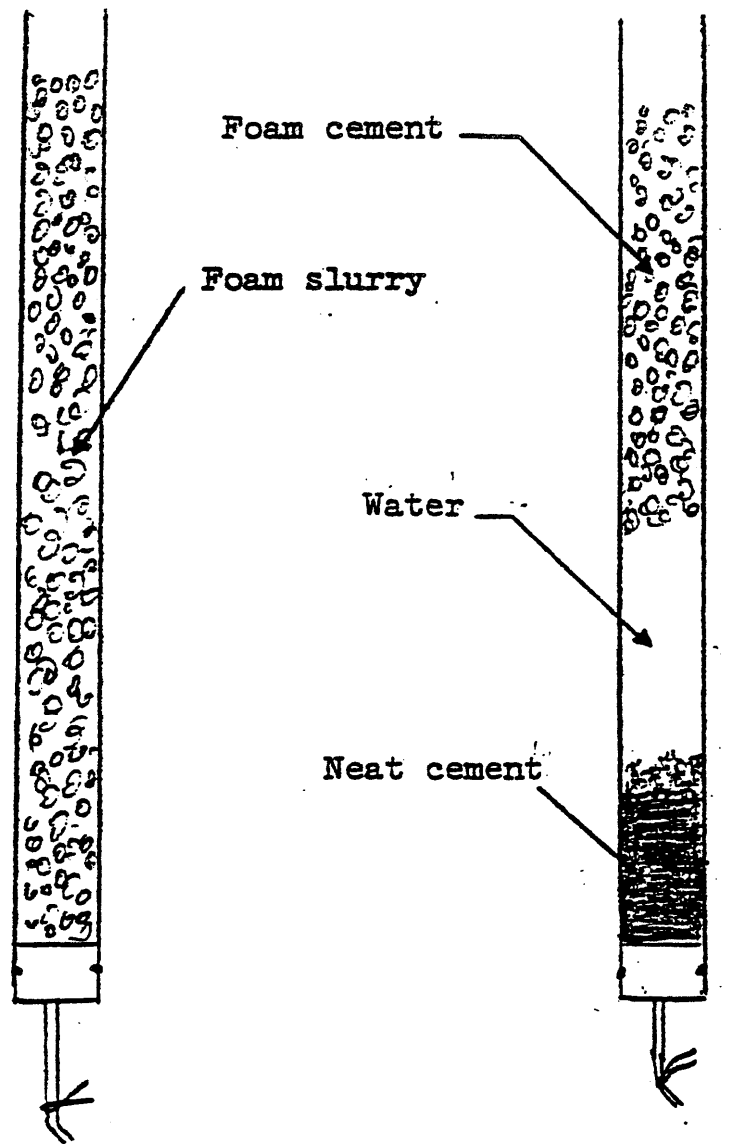


Fig. 20. Typical Foam Stability Analysis.



Instants after
injection

Two hours after
injection

Fig. 21. Ultimate Segregation.

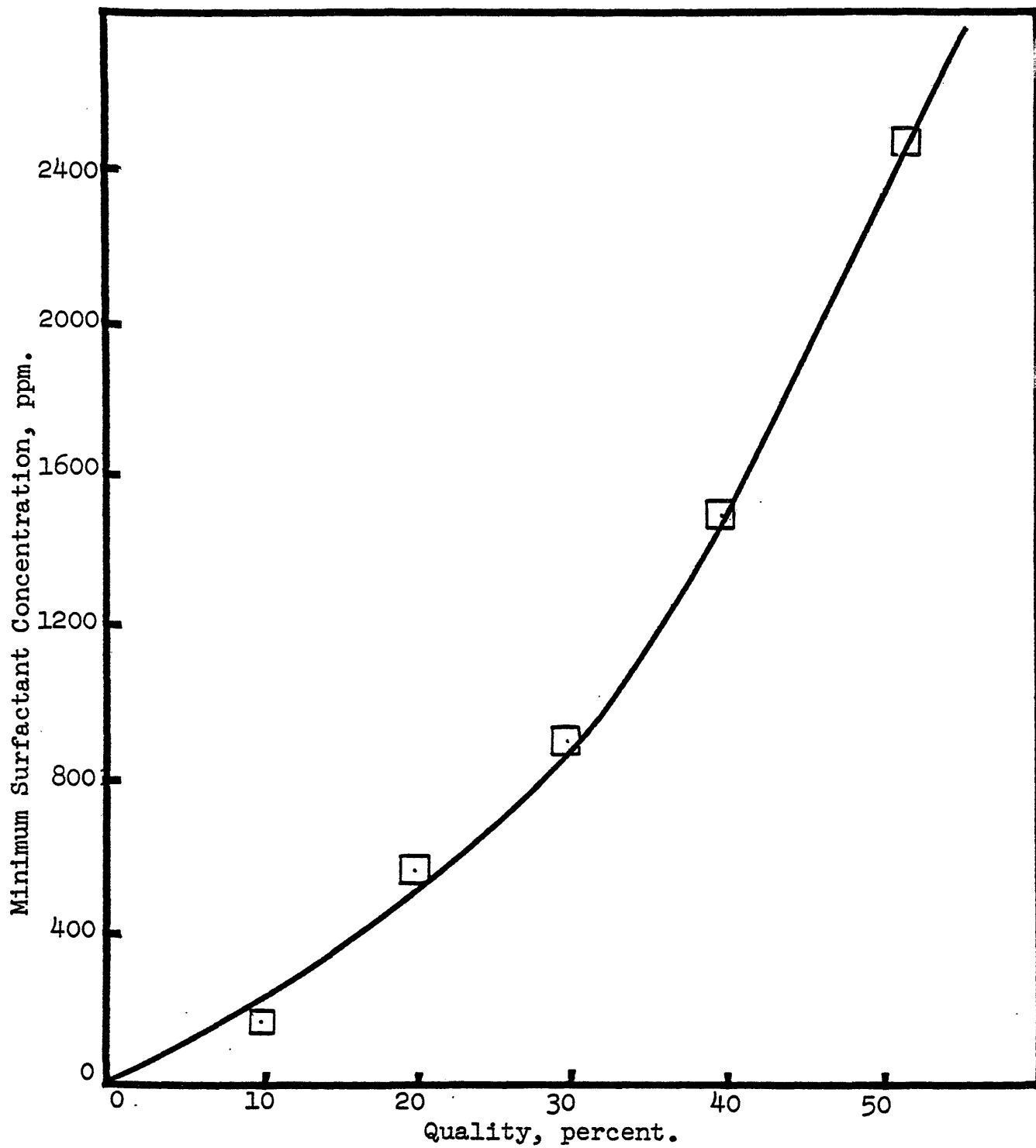


Fig. 22. Minimum Surfactant Concentration vs. Quality.

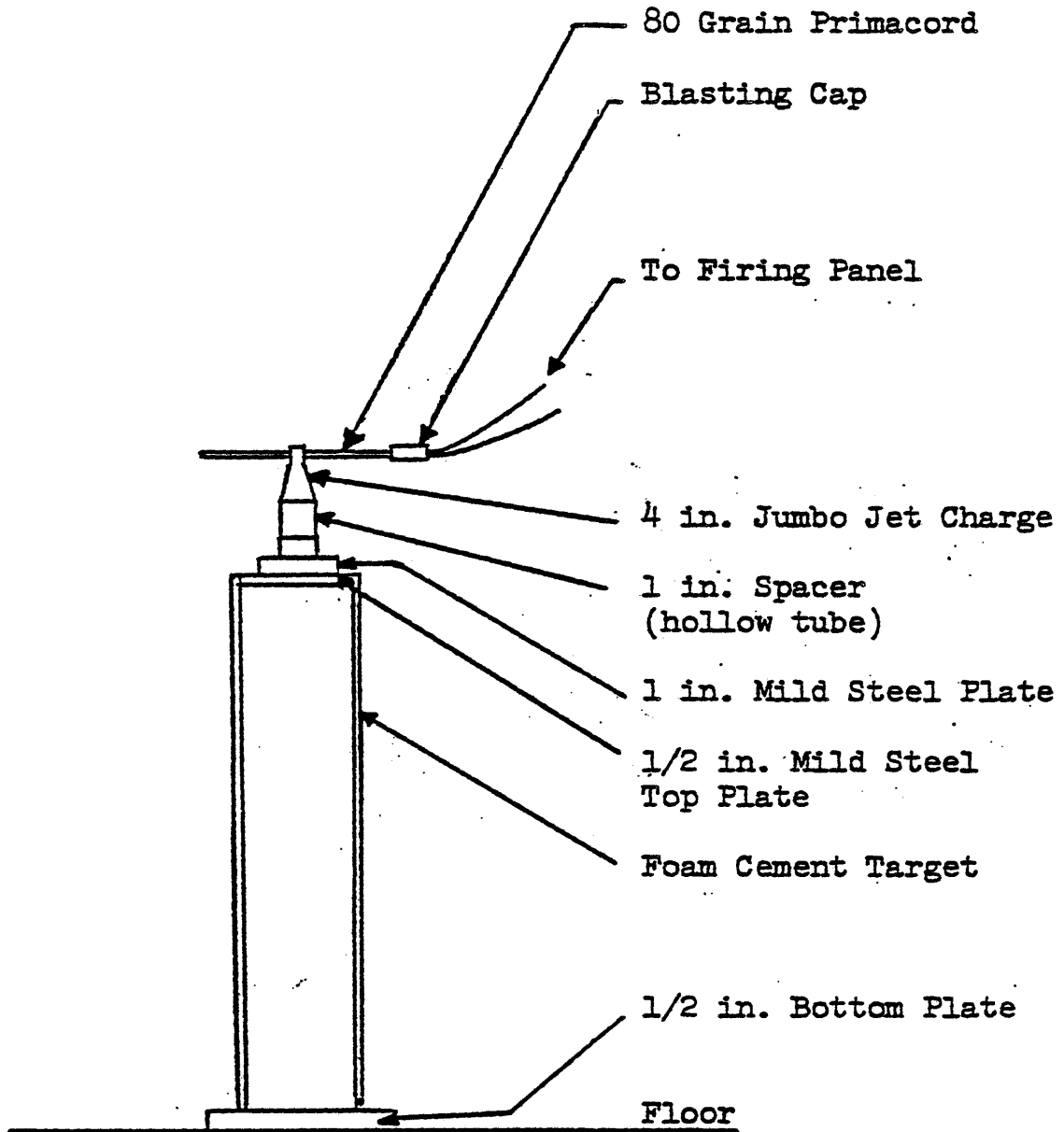


Fig. 23. Sample Perforation Setup.

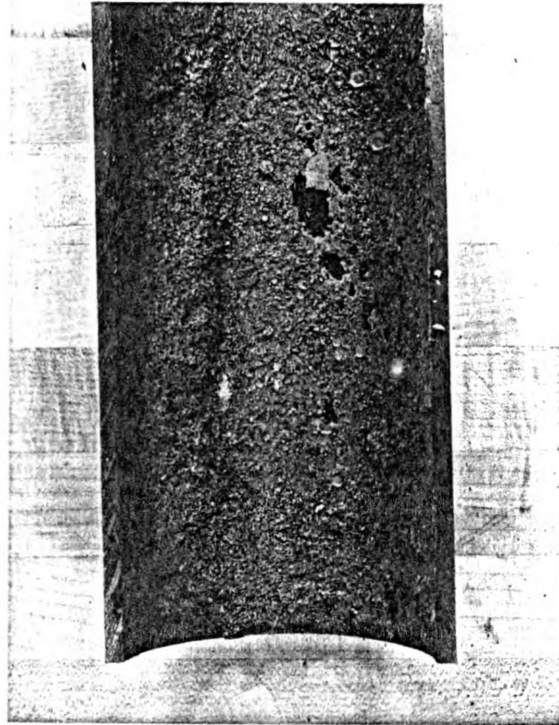


Fig. 24. Adhesion of Foam Cement to the Pipe.

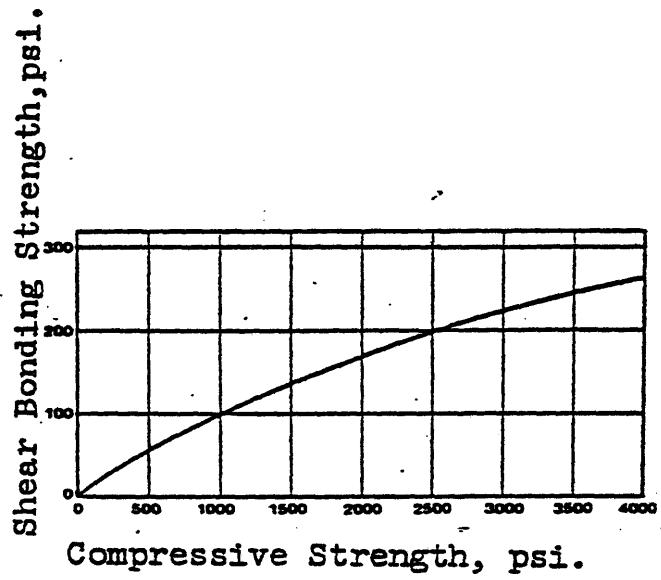


Fig. 25. Shear Bonding Strength versus Compressive Strength, (28).

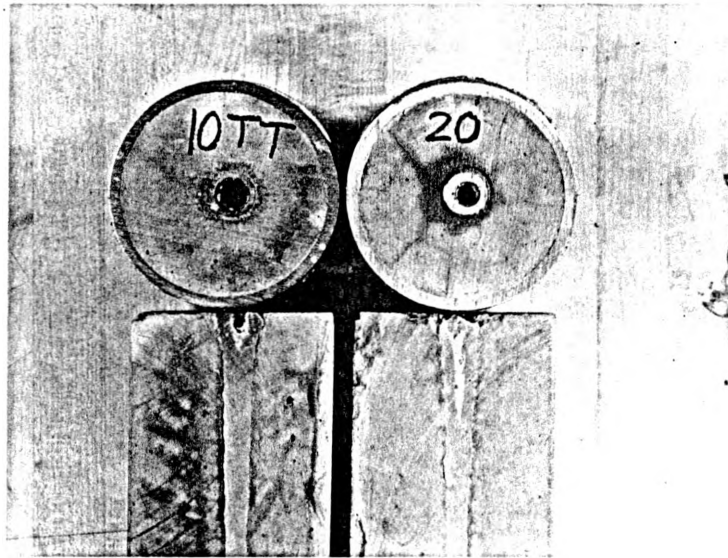


Fig. 26. Cross- Sections, Low Quality Samples.

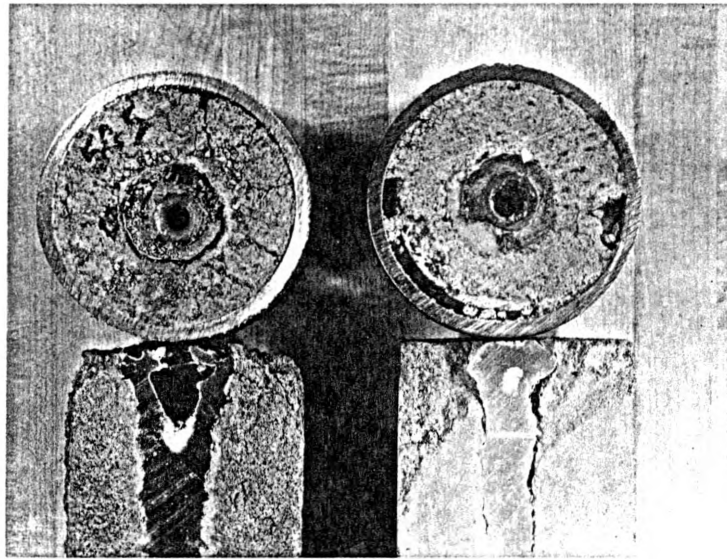


Fig. 27. Cross-Sections, High Quality Samples.

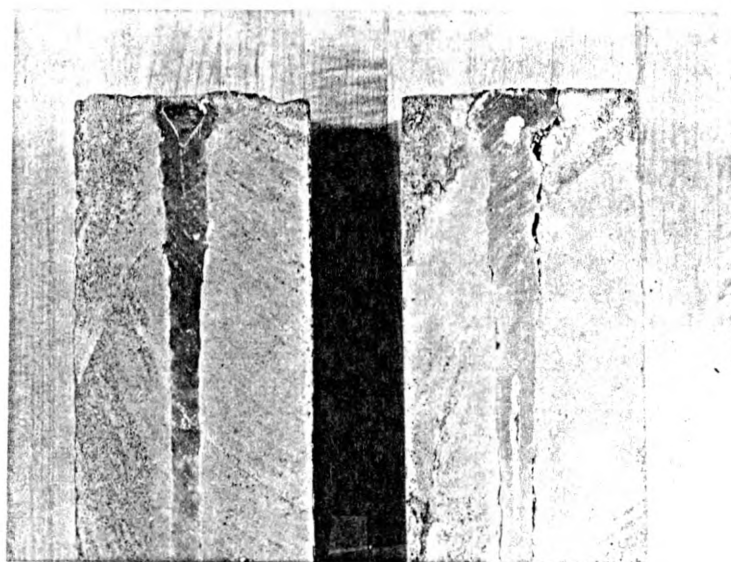


Fig. 28. Effect of Steel Plate Thickness on Perforation Diameter.

(Sample #3, left, was shot through two inches of steel, whereas sample #4, right, was shot through a one inch thick steel plate).

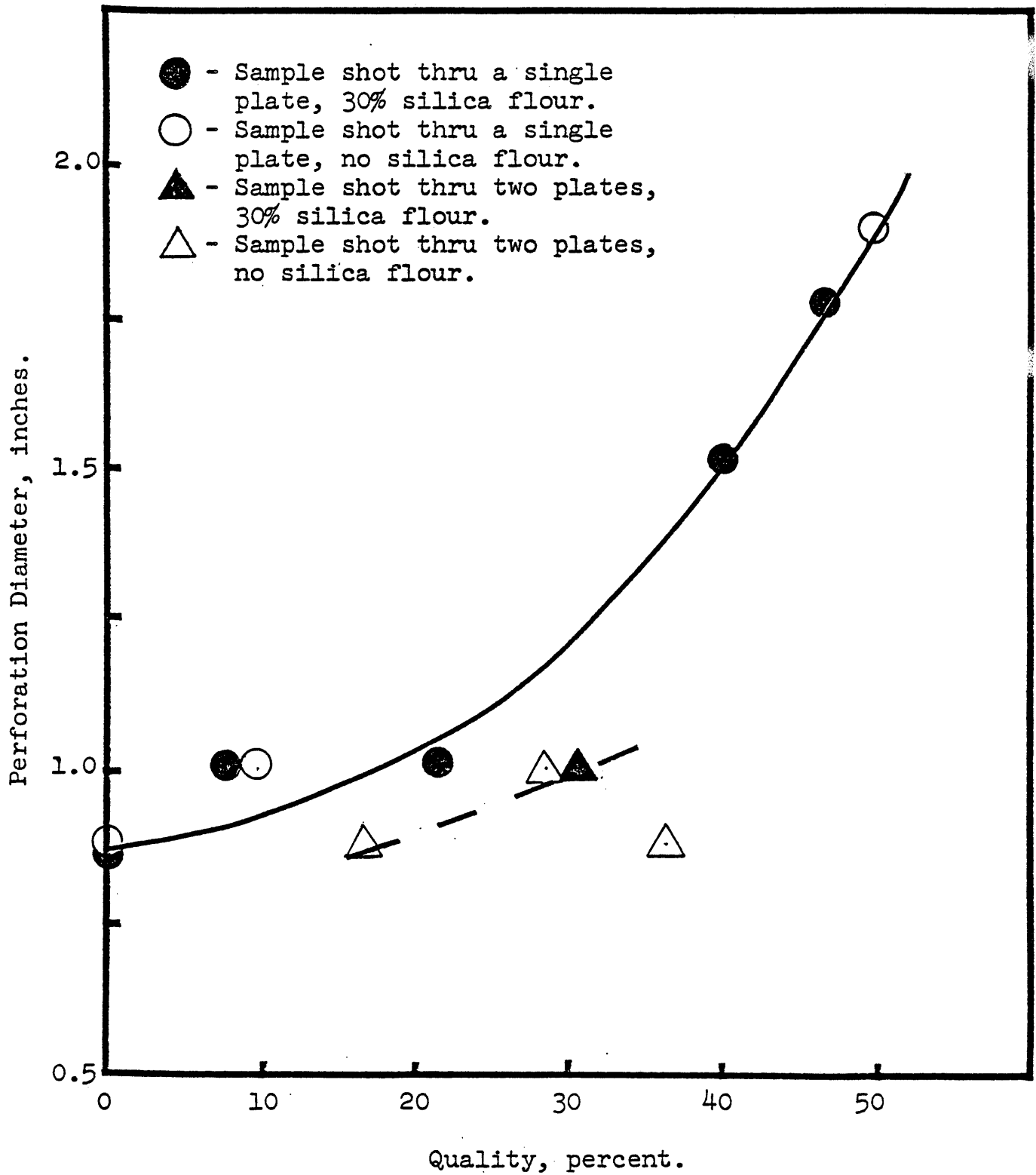


Fig. 29. Entrance Hole-Size versus Quality.



Fig. 30. Bottom Plate of Sample #1.

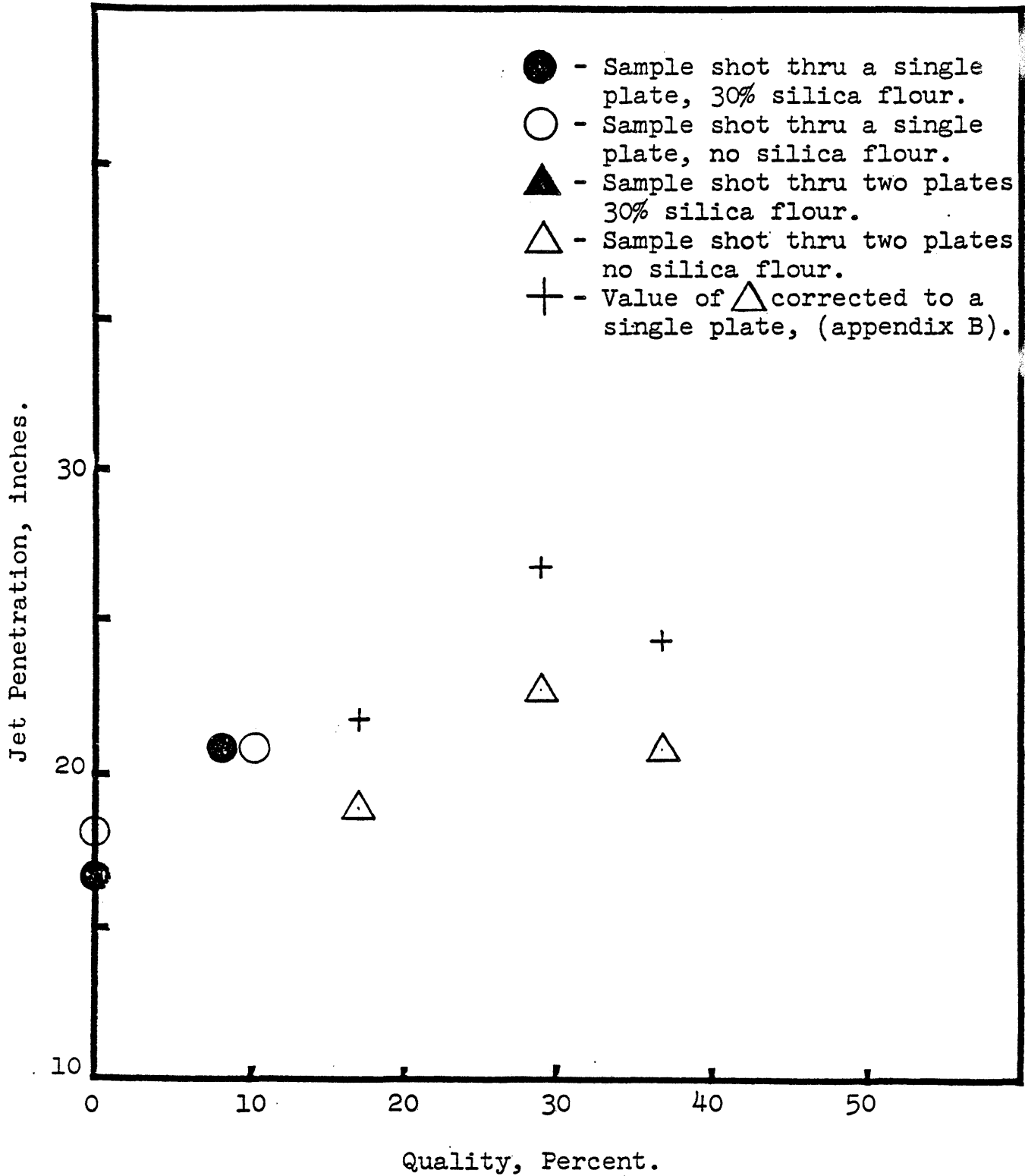


Fig. 31. Jet Penetration versus Quality.

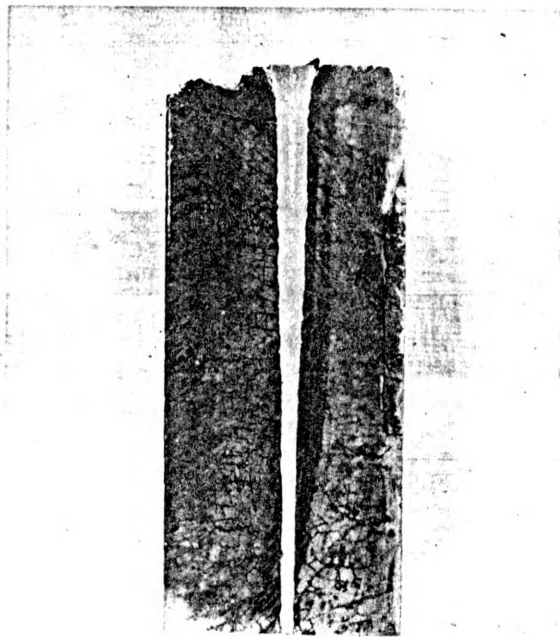
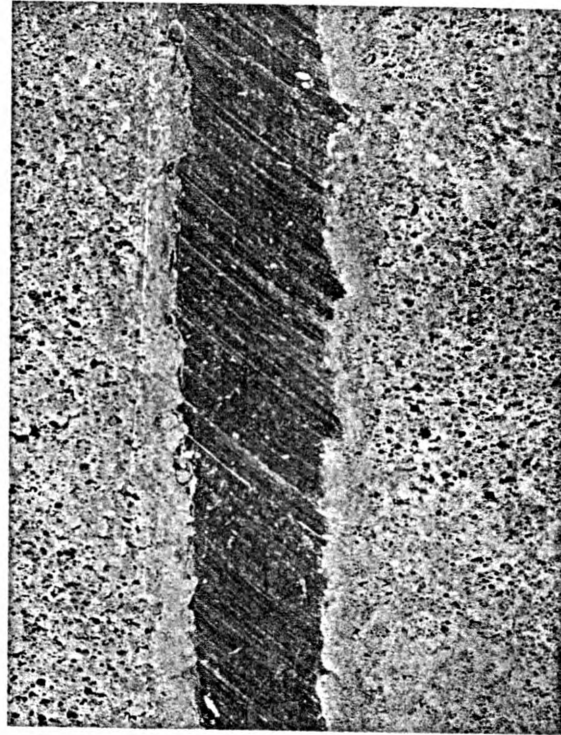


Fig. 32. Cross- Section, Neat Cement.
(Note the network of fine fractures)



(a)



(b)

Fig. 33. Cross-Section, Fifty percent Quality.

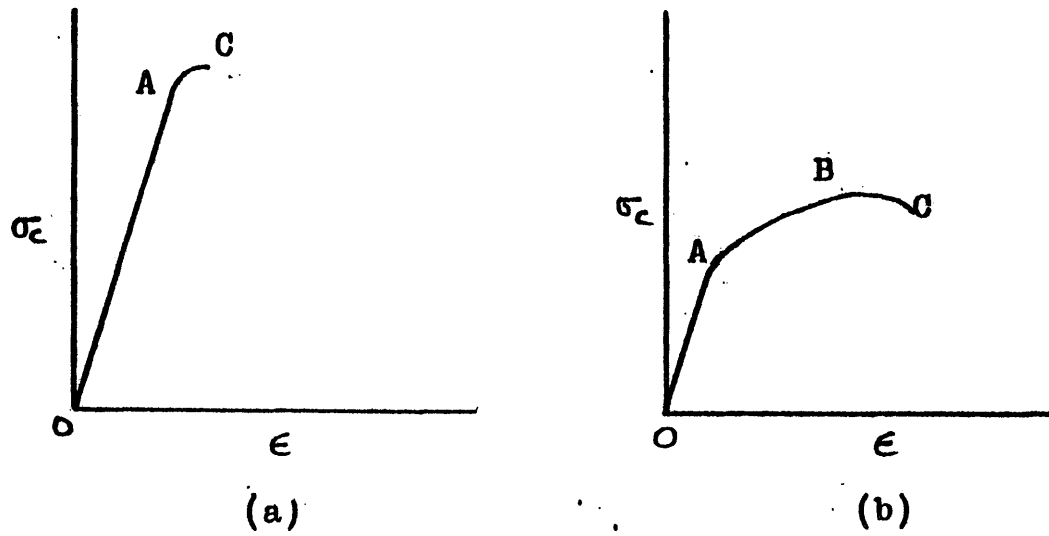
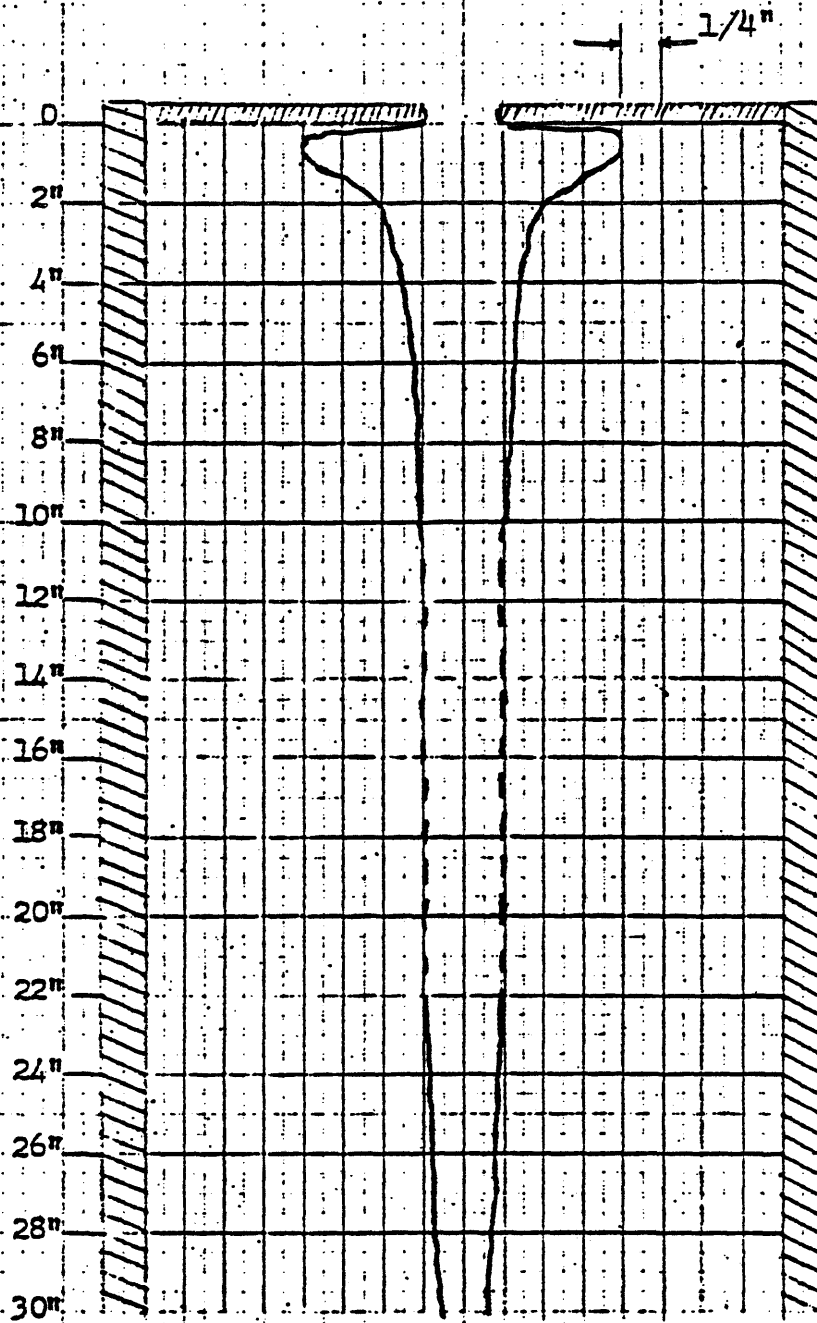


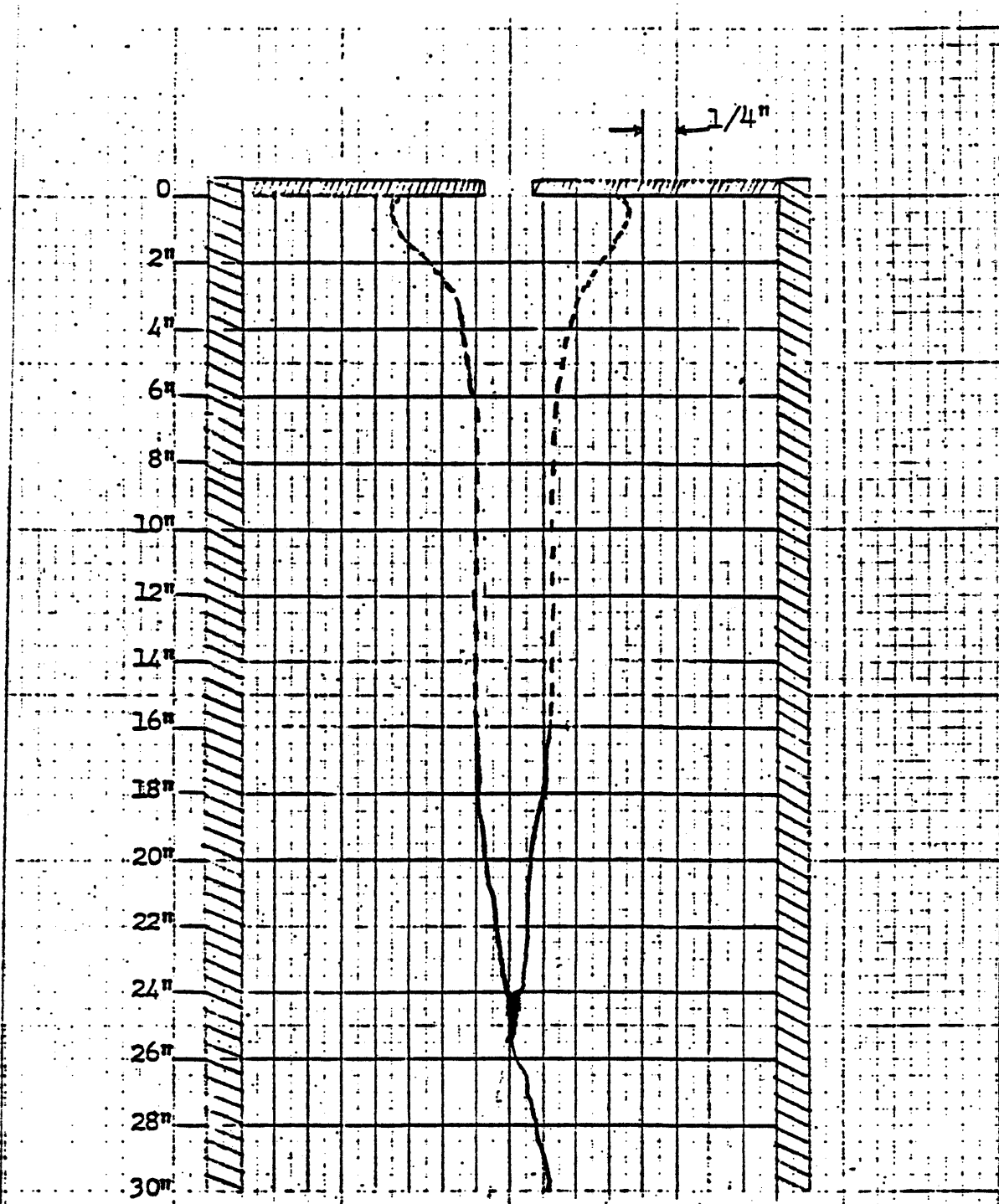
Fig. 34. Probable Stress-Strain Curves for Neat Cement (a) and Foam Cement (b).



Quality 50%

Composition 0% Silica flour

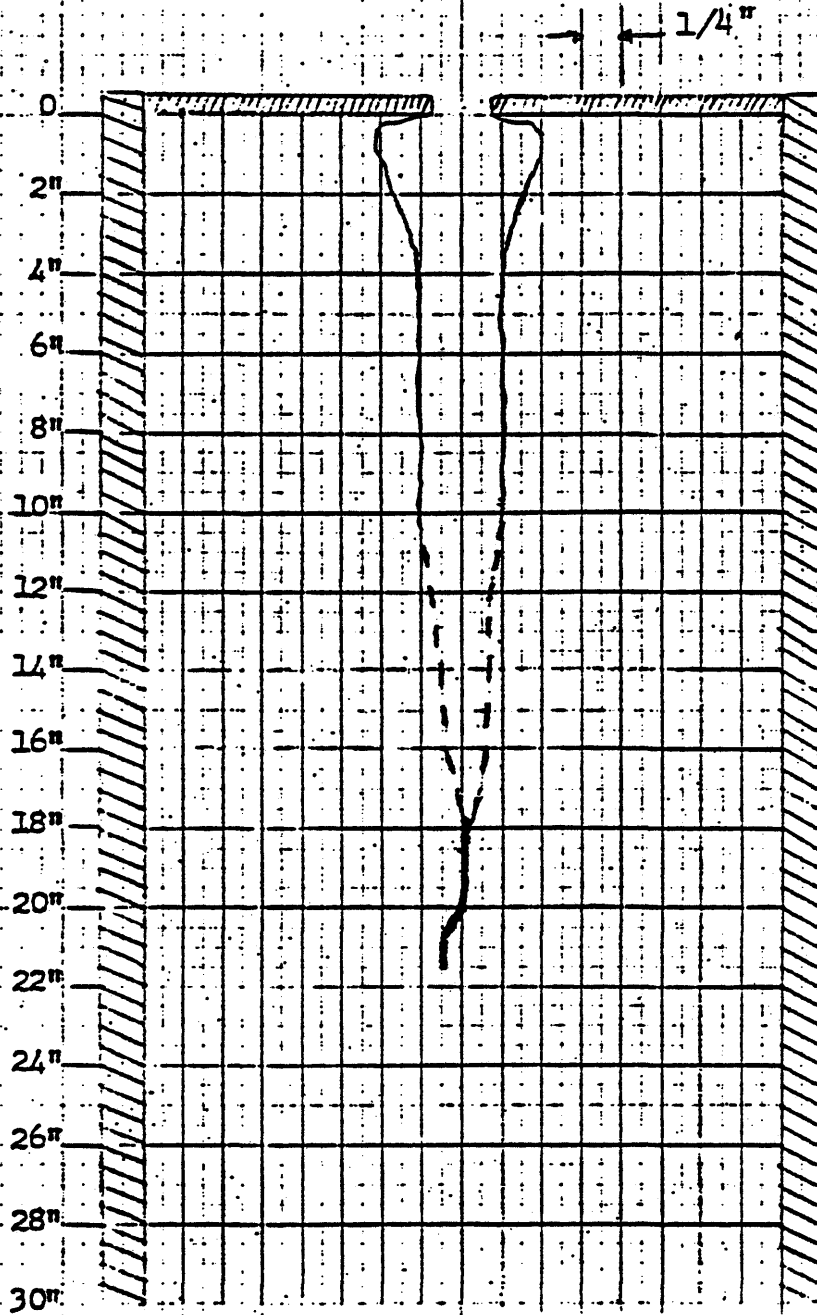
Fig. 35. Cross section, Sample #1.



Quality 47%

Composition 30% Silica flour

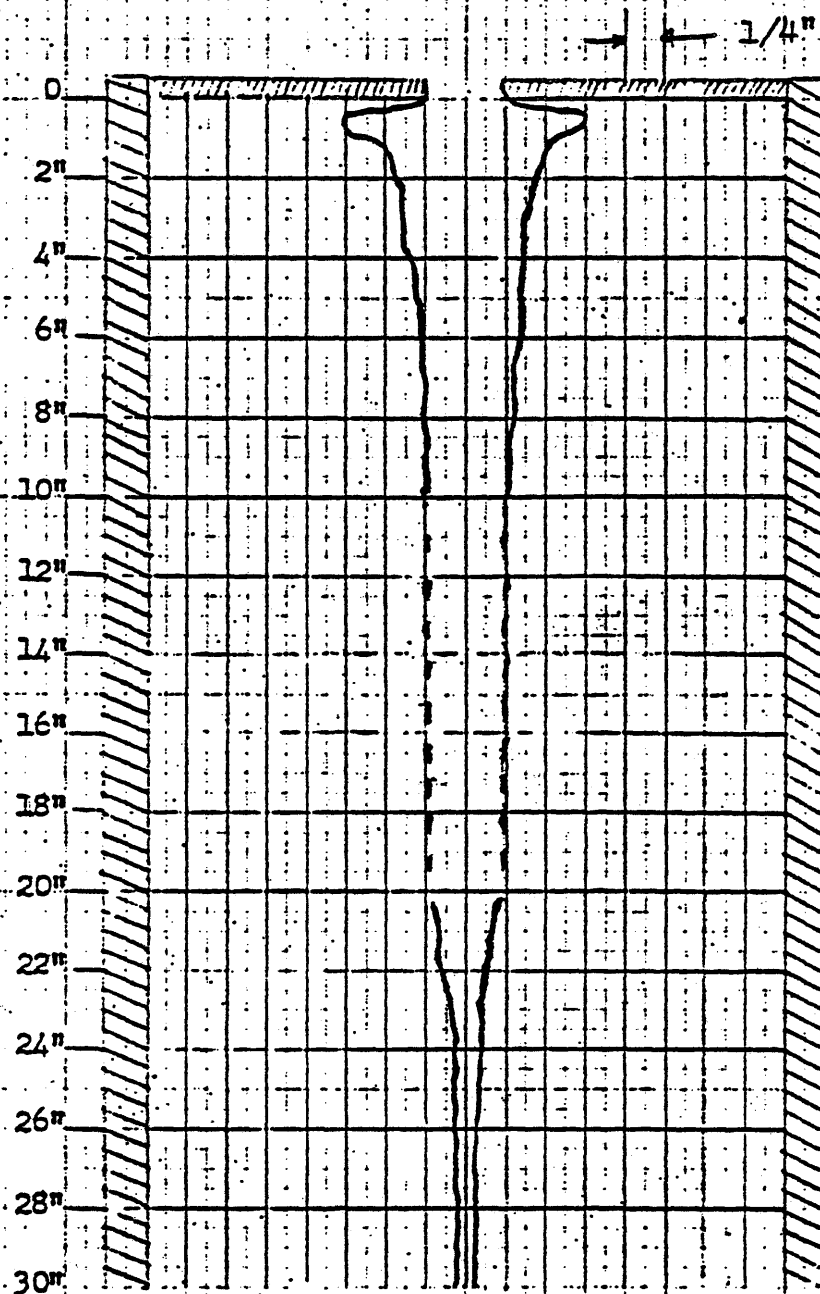
Fig. 36. Cross Section, Sample #2.



Quality 37%

Composition 0% Silica flour

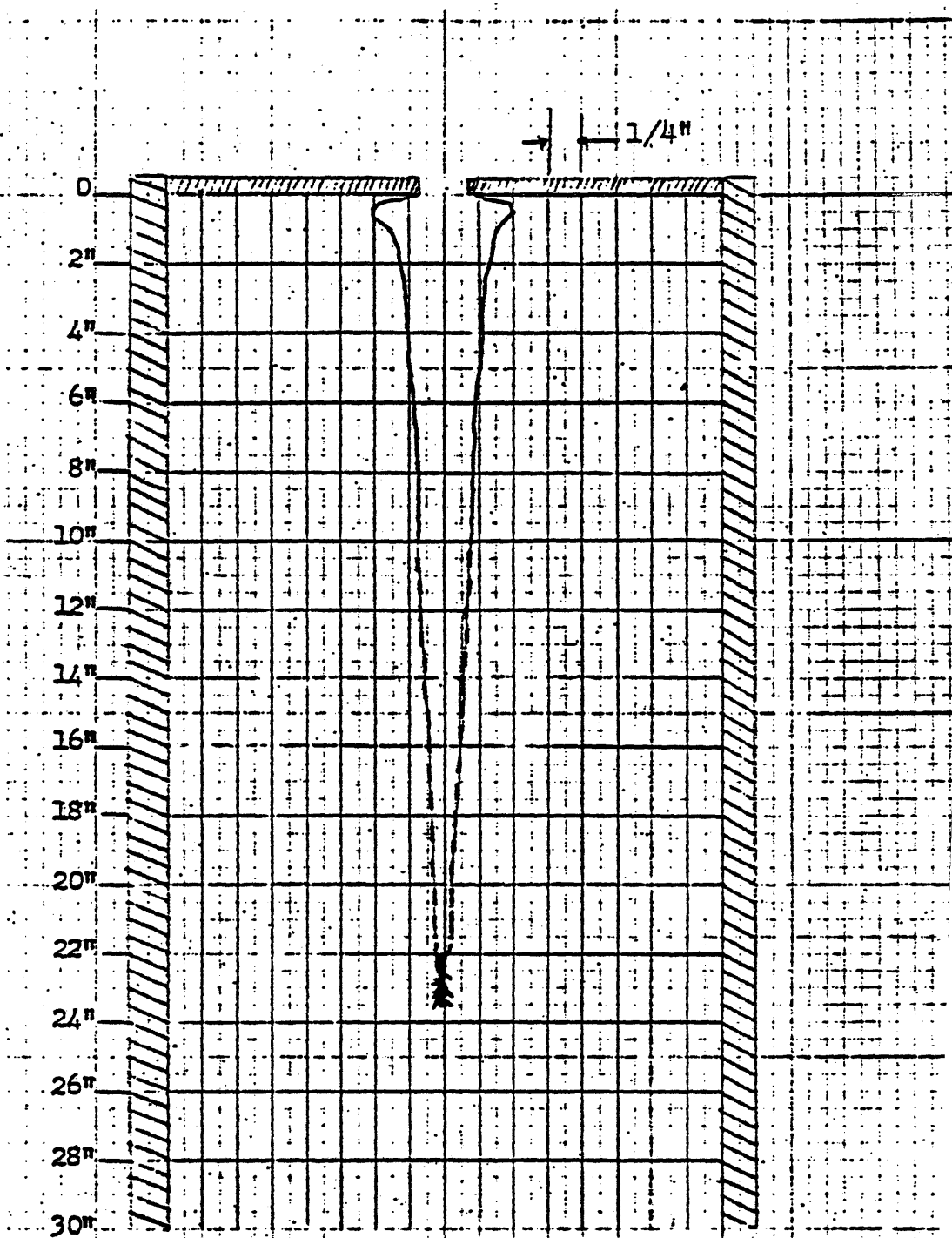
Fig. 37. Cross Section, Sample #3.



Quality 41%

Composition 30% Silica flour

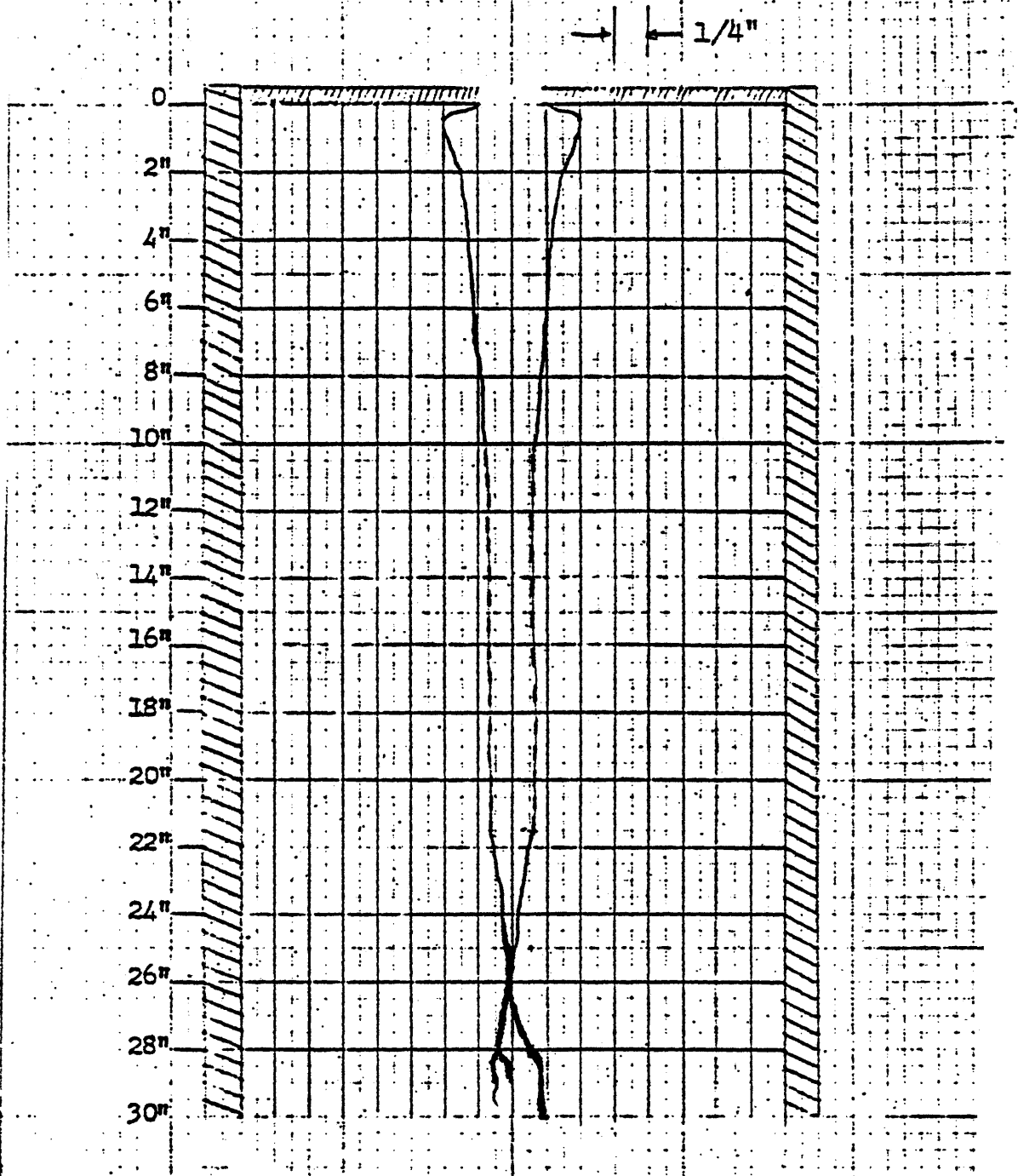
Fig. 38. Cross section, Sample #4.



Quality 29%

Composition 0% Silica flour

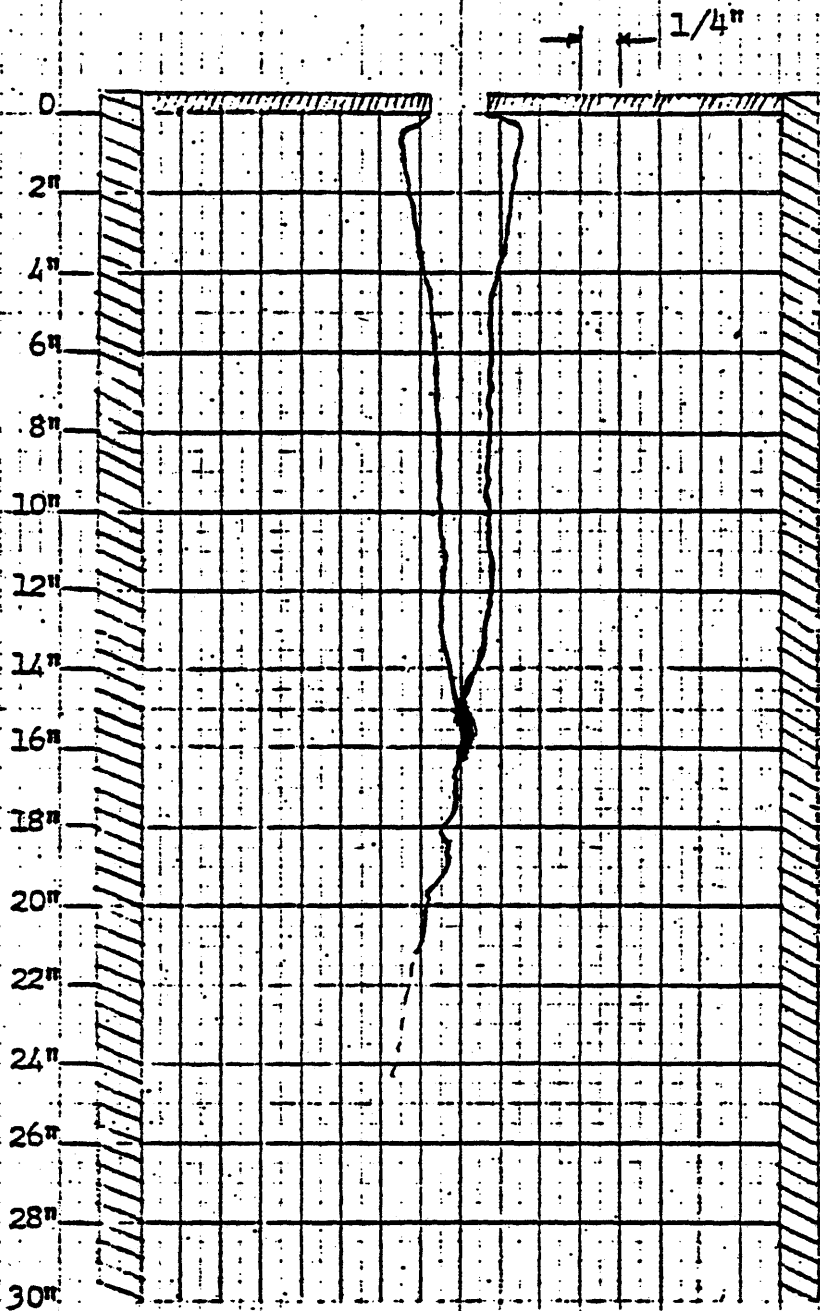
Fig. 39. Cross section, Sample #5.



Quality 31%

Composition 30% Silica flour

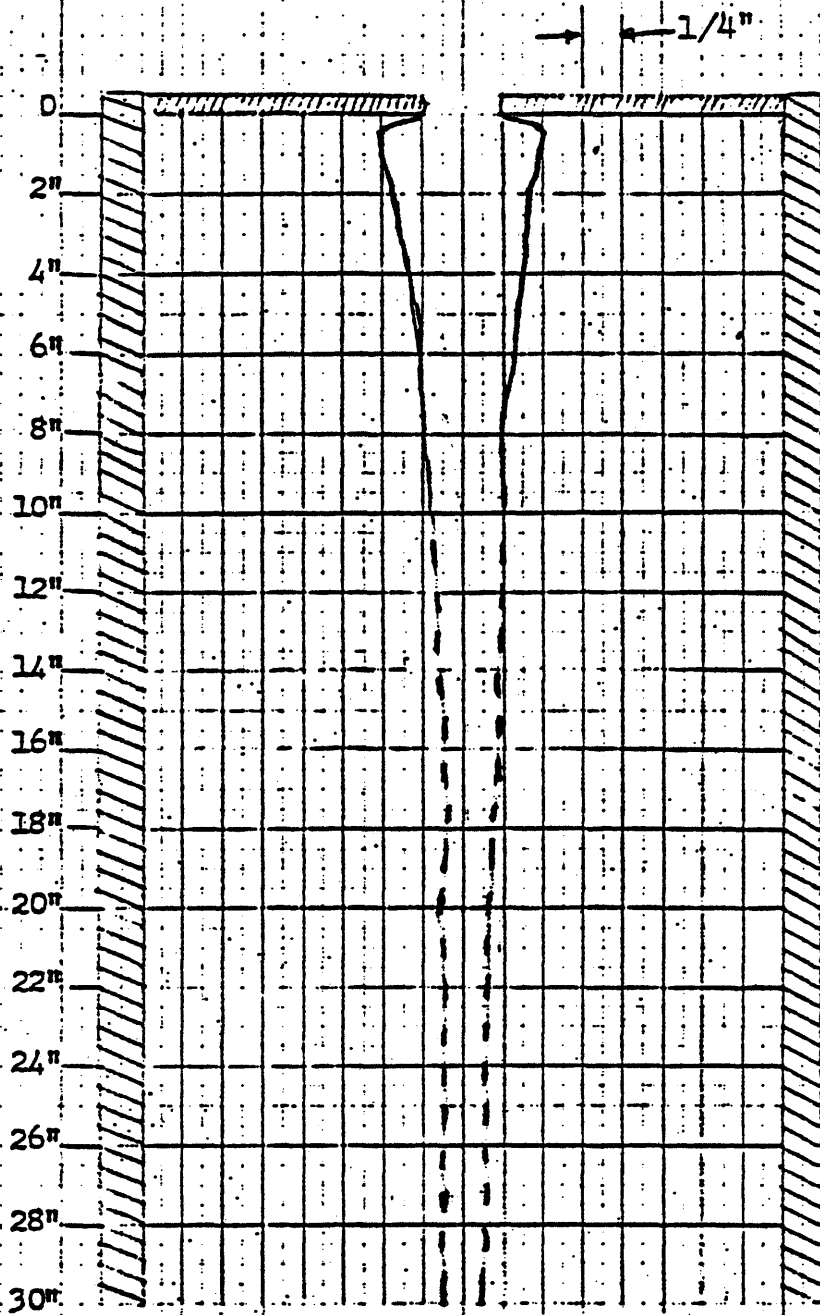
Fig. 40. Cross section, Sample #6.



Quality 17%

Composition 0% Silica flour

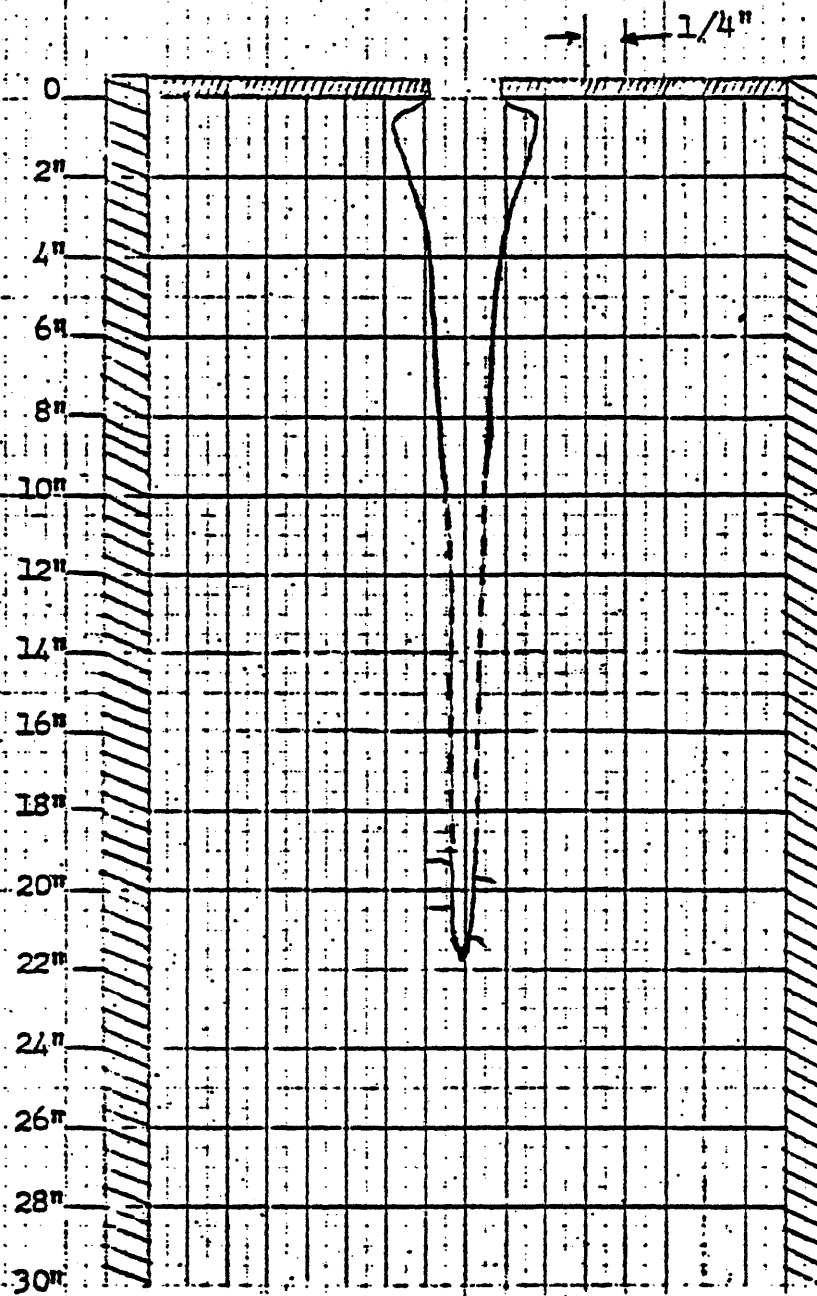
Fig. 41. Cross section, Sample #7.



Quality 22%

Composition 30% Silica flour

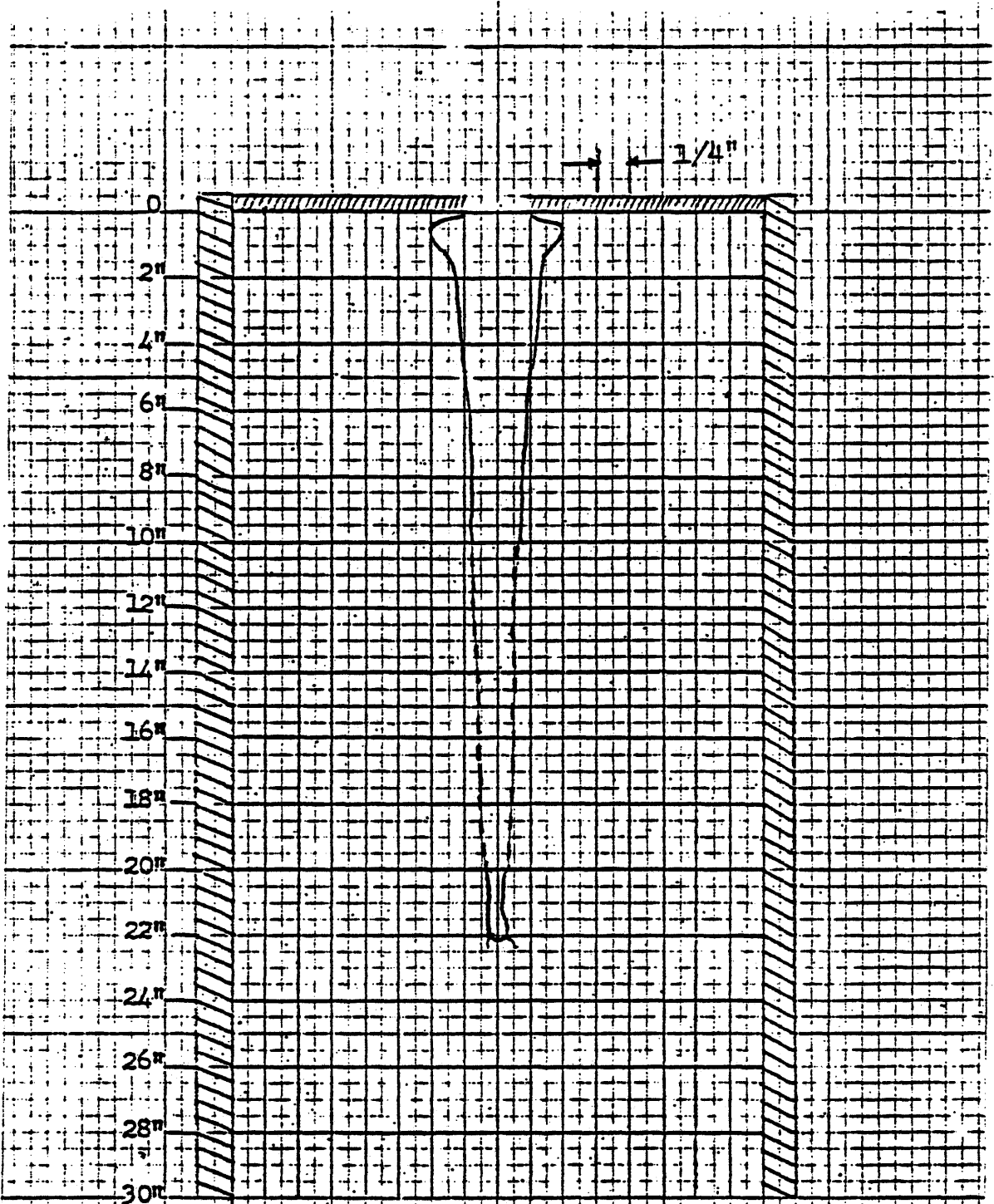
Fig. 42. Cross section, Sample #8.



Quality 10%

Composition 0% Silica flour

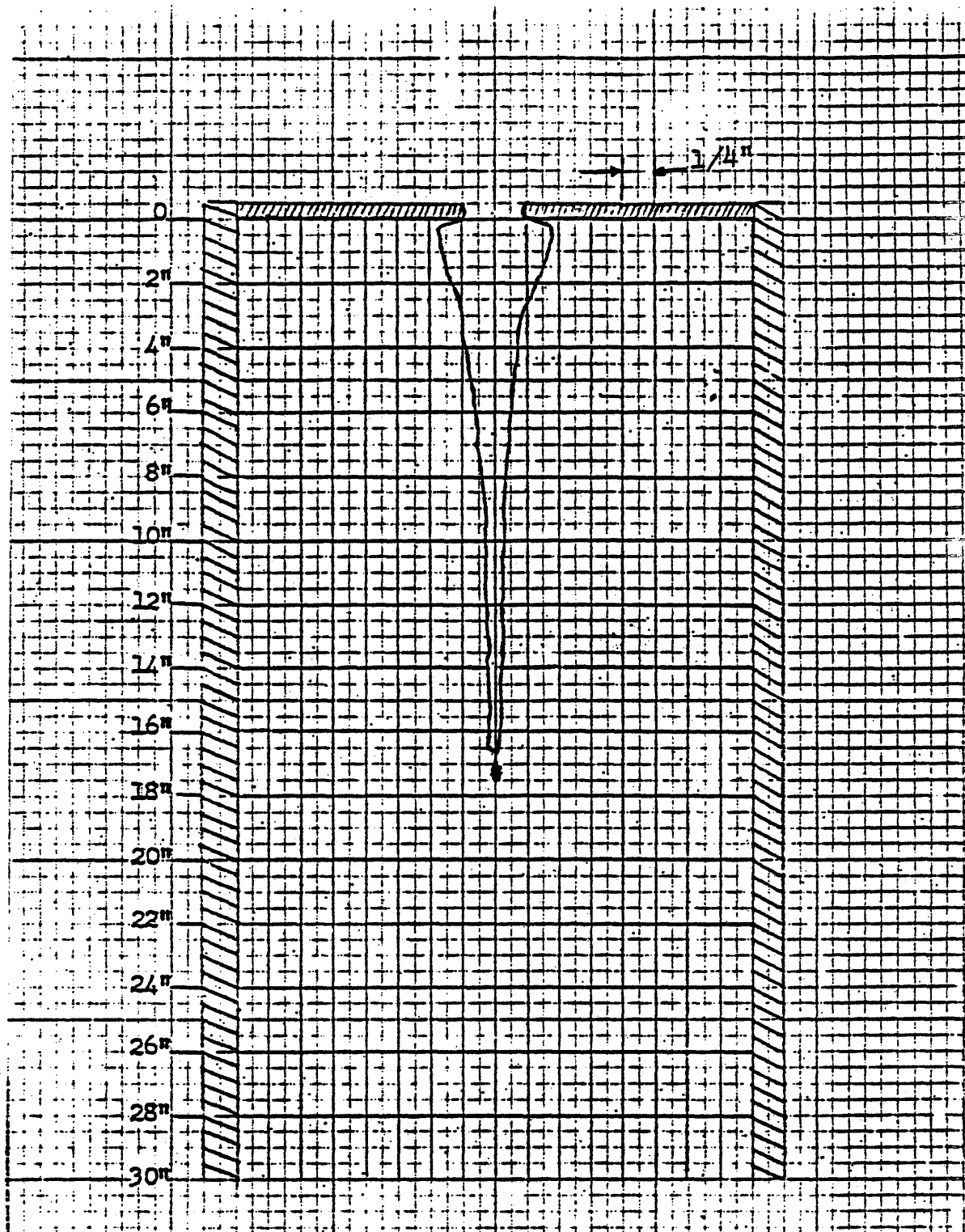
Fig. 43. Cross section, Sample #9.



Quality 8%

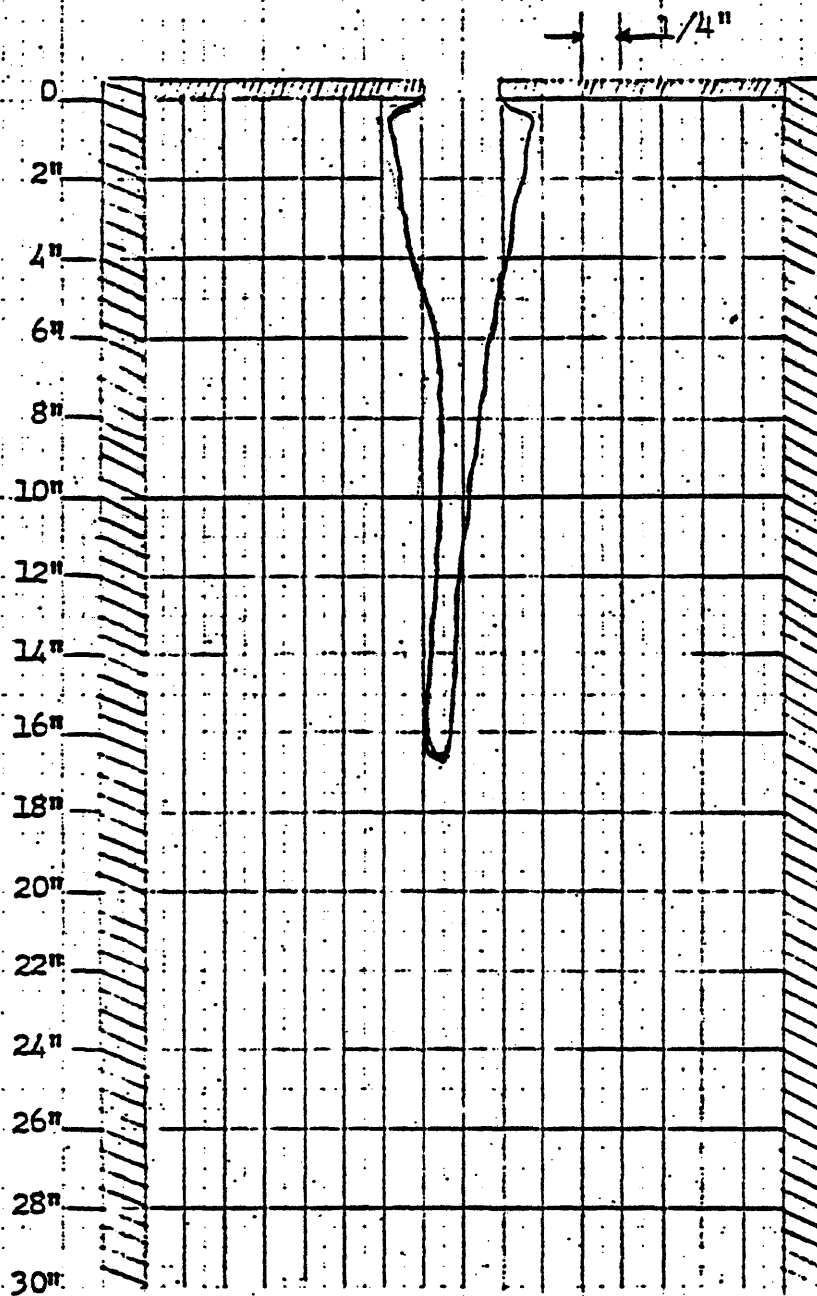
Composition 30% Silica flour

Fig. 44. Cross section, Sample #10.



Quality	0%
Composition	0% Silica flour

Fig. 45. Cross section, Sample #11.



Quality 0%

Composition 30% Silica flour

Fig. 46. Cross section, Sample #12.

TABLE 1

Sieve Analysis.

(U.S. Standard Sieve Series)
ASTM Designation C 33-67

WASHED RIVER SAND

Sieve	Percent Passing
3/8 in. (9.51 mm)	100
No. 4 (4.76 mm)	95-100
No. 8 (2.38 mm)	80-100
No. 16 (1.19 mm)	50-85
No. 30 (.595 mm)	25-60
No. 50 (.297 mm)	10-30
No. 100 (.149 mm)	2-10

TABLE 2

Typical Non-Homogeneous Batch.

Mixed: 12/5/77

Analyzed: 12/6/77

Intended quality: 50%

Mixture: Class G

Density at 0% quality: 1.83 gm/cc

<u>Sample#</u>	<u>Weight (gms)</u>	<u>Quality (%)</u>
B1*		
B2	97	73
B3	134	63
B4	153	58
B5	192	48
B6	195	47
B7	184	50
B8	217	41
B9	222	39
B10	224	39
B11	247	33
B12	251	31

* Sample caved in

TABLE 3

Typical Homogeneous Batch

Mixed: 12/19/77

Analyzed: 12/20/77

Intended quality: 30%

Mixture: Class G

Density at 0% quality: 1.83 gm/cc.

<u>Sample#</u>	<u>Weight (gms)</u>	<u>Quality (%)</u>
1B	344	31
2B	359	28
3B	359	28
4B	353	29
5B	345	31
6B	352	30
7B	352	30
8B	350	30
9B	343	31
10B	347	31
11B	351	30
12B	350	30

TABLE 4

Typical Unstable Foam.

Mixed: 11/28/77

Analyzed: 12/2/77

Intended quality: 30%

Mixture: Class G

Density at 0% quality: 1.82 gm/cc

Sequence: Top - Bottom

<u>Sample#</u>	<u>Weight (gms)</u>	<u>Volume (cc)</u>	<u>Density (gm/cc)</u>	<u>Quality (%)</u>
D1	61	64.2	.95	48
D2	64	64.2	1.00	45
D3	70	64.2	1.09	40
D4	77	64.2	1.20	34
D5	81	63.0	1.29	29
D6	81	61.3	1.32	27
D7	85	64.2	1.33	27

TABLE 5
Typical Stable Foam

Mixed: 12/19/77

Analyzed: 12/24/77

Intended quality: 25%

Mixture: Class G

Density at 0% quality 1.82 gm/cc

Sequence: Bottom - Top.

<u>Sample#</u>	<u>Weight (gms)</u>	<u>Volume (cc)</u>	<u>Density (gm/cc)</u>	<u>Quality (%)</u>
1	52	37.3	1.39	24
2A	54	38.6	1.40	24
3A	54	38.6	1.37	26
4A	53	38.6	1.40	24
5A	53	37.3	1.42	23
6A	53	37.3	1.42	23
7A	53	38.6	1.37	26
8A	53	38.6	1.37	26
9A	53	38.6	1.37	26
10A	53	8.6	1.37	26
11A	68	50.2	1.35	25

TABLE 6

Homogeneity Check on Foam Cement Samples, 50% Quality

Mixture: Class G Cement and Water

Surfactant concentration 2,400 ppm

Shaking time 30 minutes

Date 2/5/77

<u>Sample #</u>	<u>Density (ppg)</u>	<u>Quality (%)</u>
1	7.9	50
2	8.0	49
3	7.9	50
4	---	---
	<hr/>	<hr/>
Average	7.93	50

TABLE 7

Homogeneity Check on Foam Cement Samples, 50% Quality

Mixture: Class G Cement, water and Silica flour

Surfactant concentration 2,400 ppm

Shaking time 30 minutes

Date 2/5/77

88

<u>Sample #</u>	<u>Density (ppg)</u>	<u>Quality (%)</u>
1	8.2	47
2	8.3	47
3	8.2	47
4	8.2	47
Average	<u>8.18</u>	<u>47</u>

TABLE 8

Homogeneity Check on Foam Cement Samples, 40% Quality

Mixture: Class G Cement and Water

Surfactant concentration 1,600 ppm

Shaking time 30 minutes

Date 2/5/77

<u>Sample #</u>	<u>Density (ppg)</u>	<u>Quality (%)</u>
1	9.8	38
2	9.9	37
3	10.1	36
4	10.1	36
Average	9.98	37

TABLE 9

Homogeneity Check on Foam Cement Samples, 40% Quality

Mixture: Class G Cement, water and Silica flour

Surfactant concentration 1,600 ppm

Shaking time 30 minutes

Date 2/5/77

<u>Sample #</u>	<u>Density (ppg)</u>	<u>Quality (%)</u>
1	9.0	42
2	9.3	40
3	9.3	40
4	9.2	41
Average	9.2	41

78

T-2069

TABLE 10

Homogeneity check on Foam Cement Samples, 30% Quality

Mixture: Class G Cement and Water

Surfactant concentration 900 ppm

Shaking time 30 minutes

Date 2/5/77

<u>Sample #</u>	<u>Density (ppg)</u>	<u>Quality (%)</u>
1	11.3	28
2	11.2	29
3	11.3	28
4	11.1	30
	<hr/>	<hr/>
Average	11.23	29

TABLE 11

Homogeneity Check on Foam Cement Samples, 30% Quality

Mixture: Class G Cement, water and Silica flour

Surfactant concentration 900 ppm

Shaking time 30 minutes

Date 2/5/77

<u>Sample #</u>	<u>Density (ppg)</u>	<u>Quality (%)</u>
1	11	29
2	10.7	31
3	10.7	31
4	10.5	33
	<hr/>	<hr/>
Average	10.73	31

8

T-2069

TABLE 12

Homogeneity Check on Foam Cement Samples, 20% Quality

Mixture: Class G Cement and Water

Surfactant concentration 600 ppm

Shaking time 30 minutes

Date 2/6/77

<u>Sample #</u>	<u>Density (ppg)</u>	<u>Quality (%)</u>
1	13.2	16
2	13.3	16
3	13.0	18
4	13.2	16
	<hr/>	<hr/>
Average	13.18	17

TABLE 13

Homogeneity Check on Foam Cement Samples, 20% Quality

Mixture: Class G Cement, water and Slica flour

Surfactant con entration 600 ppm

Shaking time 15 minutes

Date 2/6/77

Sam

∞
∞

<u>Sample #</u>	<u>Density (ppg)</u>	<u>Quality (%)</u>
1	12.2	22
2	12.3	21
3	12.1	22
4	12.2	22
	<hr/>	<hr/>
Average	12.20	22

TABLE 14

Homogeneity Check on Foam Cement Samples, 10% Quality

Mixture: Class G Cement and Water

Surfactant concentration 200 ppm

Shaking time 15 minutes

Date 2/6/77

89

<u>Sample #</u>	<u>Density (ppg)</u>	<u>Quality (%)</u>
1	14.1	11
2	14.2	10
3	14.2	10
4	14.2	10
	<hr/>	<hr/>
Average	14.18	10

SAMPLE 15

Homogeneity Check on Foam Cement samples, 10% Quality

Mixture: Class G Cement, water and Silica flour

Surfactant concentration 200 ppm

Shaking time 15 minutes

Date 2/6/77

96

<u>Sample #</u>	<u>Density (ppg)</u>	<u>Quality (%)</u>
1	14.3	8
2	14.4	8
3	14.2	9
4	14.3	8
	<hr/>	<hr/>
Average	14.3	8

TABLE 16

Homogeneity Check on Foam Cement Samples, 0% Quality

Mixture: Class G Cement and Water

Surfactant concentration 0 ppm

Shaking time 0 minutes

Date 2/6/77

<u>Sample #</u>	<u>Density (ppg)</u>	<u>Quality (%)</u>
1	15.8	0
2	15.8	0
3	15.7	1
4	15.8	0
	<hr/>	<hr/>
Average	15.78	0

TABLE 17

Homogeneity Check on Foam Cement Samples, 0% Quality

Mixture: Class G Cement, water and Silica flour

Surfactant concentration 0 ppm

Shaking time 0 minutes

Date 2/6/77

92

<u>Sample #</u>	<u>Density (ppg)</u>	<u>Quality (%)</u>
1	15.5	1
2	15.4	1
3	15.6	0
4	15.6	0
	<hr/>	<hr/>
Average	15.53	0

TABLE 18

Summary of Target Samples Conditions.

<u>Sample#</u>	<u>Quality(%)</u>	<u>Silica flour in composition</u>	<u>Inches of mild steel shot through</u>	<u>Max hole diameter</u>	<u>Max Penetration</u>
1	50	no	1	1 9/8	Max*
2	47	yes	1	1 3/4	Max*
3	37	no	2	7/8	21
4	41	yes	1	1 1/2	Max*
5	29	no	2	1	23
6	31	yes	2	1	Max*
7	17	no	2	7/8	15
8	22	yes	1	1	Max*
9	10	no	1	1	21
10	8	yes	1	1	21
11	0	no	1	7/8	18
12	0	yes	1	7/8	16

* more than 30 inches.

REFERENCES

1. Meade, R.K., Portland Cement, The Chem. Pub. Co., 1926.
2. Eckel, C.E., Cements, Limes and Plasters, John Wiley and Sons, Inc., 1928. pp 1-16.
3. Valore, R.C., "Foam and Gas Concretes," Structural Foams, Building Research Institute, Publication 892, 1960. pp 26
4. Aldrich, C.A. and Mitchell, B.J., "Strength, Permeability, and Porosity of Oilwell Foam Cement," Journ. of Eng. for Ind., Vol. 98, No.3 August 1976.
5. Bikerman, J.J. Foams, Springer - Verlag, New York, 1973. pp 2
6. Al Mashat, "Rheology of Foam Cement," Doctoral Thesis, Colorado School of Mines, T 1887, 1976.
7. Richardson, E.G., J. of Coll. Sci., Vol. 5, 1950, pp. 404.
8. Becher, P., Emulsions: Theory and Practice, Reinhold Pub. Co., 2nd Ed., 1965. pp 279.
9. Rumscheidt, F.D. and Mason, S.G., J. Colloid. Sci., Vol. 17, 1962. pp 260
10. Taylor, G.I., Proc. Roy. Soc. (London), Vol. A146, 1934, pp 501.
11. Ottewill, R.H., J. Chem. Soc. Faraday Trans., 1976, pp 379
12. Derjacvin, B.V. and Landau, L., Acta Physicochem. URSS, Vol. 14, 1941, pp 633
13. Verwey, E.J.W., and Overbeek, J.T.G., Theory of the the Stability of Lyophobic Colloids, Elsevier, Amsterdam, 1948.
14. Pickering, S.U., J. Soc. Chem. Ind., Vol. 29, 1910, pp.129
15. Mukerjee, L.N. and Srivastava, S.N., Kolloid - Z Vol. 147, 1956, pp 146.
16. Bikerman, J.J., Foams, Springer - Verlag, New York, 1973, pp 149-157
17. Aldrich, C.S., "Strength, Permeability, and Porosity of a Porosity of a Cellular Oil Well Cement", M.S. Thesis Colorado School Of Mines, T - 1604, 1974
18. Slattery, J.P., "Compressive and Tensile Strengths and Setting Times of Foam Cement with Common Additives", M.S. Thesis Colorado School of Mines, T 1832, 1976.
19. Detkov, V.P. and Sabrizyanov, A.K., "The use of Aerated Plugging Suspensions for Well Cementation", Neftyanoe Khozvaistvo, Vol. 5, May 1976.

20. Pakbaz, E., "Long Term Strength and Permeability of Foam Cement at Elevated Temperatures," Doctoral Thesis, Colorado School of Mines, T-2058, 1978.
21. "Perforating Technology" Dresser Atlas Division Dresser Industries, Inc.
22. Birkoff, McDougall, Pugh, and Taylor, J. Appl. Phys. Vol. 19, 1948, pp 563.
23. Pugh, Eichelberger and Rostoker, "Theory of Jet Formation by Charges with Lined Conical Cavities", J. Appl. Phys., Vol. 23, 1952, pp 532.
24. Thompson, G.D., "Effects of Formation Compressive Strength on Perforator Performance", Drill. and Prod. Practice, API, 1962, pp 191
25. API Rp 43, "API Recommended Practice standard Procedure for evaluation of Well Perforators", 3rd Ed., Oct. 1974
26. Becher, P., Emulsions: Theory and Practice, 2nd Ed, Reinhold Pub. Co., 1965, pp 95
27. Parker, Clement, Beirute, "Basic Cementing", Oil and Gas J., Vol. 75, No. 8, Feb. 21, 1977, pp. 61.
28. Smith, D.K., Cementing, SPE Monograph, Vol. 4, 1976, pp.113.

APPENDIX A

A formula derived and experimentally verified is used to "roughly" estimate the amount of shear G necessary to burst a bubble of air in cement slurry. The formula was derived strictly for laminar shear flow of liquids; it will be used only for order of magnitude calculations.

$$E=1/2$$

$$Gr\eta_2/\gamma=1/2$$

thus

$$G=\gamma/2r\eta_2.$$

where

γ = Surface tension.

η_2 = Viscosity of the cement.

r = Bubble radius.

Shear rate at the wall of a pipe, in which Bingham Plastic fluid is flowing with a velocity V , is reported by Al Mashat (6) under the following form:

$$\frac{dV}{dr} = \frac{8V}{D} \quad D \text{ being the pipe's ID.}$$

Let's assume that $\frac{dV}{dr} = G$

$$\text{then } V = DG/8$$

The required flow rate to burst the air bubble is:

$$Q = AV = \pi D^3 V / 4 = D^3 G / 32$$

Replacing G by its value above

$$Q = (\pi D^3 / 32) \times (\gamma / 2r\eta_2) = (\pi D^3 \gamma) / (64\eta_2 r)$$

Numerical application:

$$D = .5 \text{ in.} = 1.27 \text{ cm.}$$

$$\gamma = 30 \text{ dynes/cm.}$$

$$\eta_2 = 20 \text{ cp or } .02 \text{ dyne}\cdot\text{sec}\cdot\text{cm}^{-2}$$

$$\text{For } r = .1 \text{ cm.}$$

$$V = 120 \text{ cm/sec or } 3.9 \text{ ft/sec.}$$

$$\text{For } r = .01 \text{ cm.}$$

$$V = 39 \text{ ft/sec.}, \text{ corresponding to}$$

$$Q = 24 \text{ gpm.}$$

T-2069

APPENDIX B



DRESSER ATLAS DIVISION, DRESSER INDUSTRIES, INC. P.O. BOX 6604, HOUSTON, TEXAS 77006 713 784-6011 TWX: 910-881-3708

March 21, 1978

Mr. Khaled Chekeri
Department of Petroleum Engineering
Colorado School of Mines
Golden, Colorado 80401

Dear Mr. Chekeri:

The perforating of the twelve foam cement targets has been completed and they are enroute to you at this time.

As we discussed on the telephone, some problems were encountered in scaling a jet perforator down to prevent shooting completely through the target. This was accomplished through the use of 1" mild steel plates between the charge and the target. A single 1" plate was used on all tests except #3, #5, #6 & #7, where two plates were used.

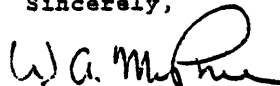
The charge used was a 4" Jumbo Jet and was shot as shown on the attached sketch. This is our premium charge and was selected because of its consistency. It will shoot 6" in mild steel, 14" in Berea sandstone (compressive strength 6000 psi to 9000 psi), and 20" in concrete (compression strength 4000 psi to 5000 psi). (See attached sheet.)

The insertion of an 1" thick steel plate between the target and the charge results in a 16.7% loss in penetrating energy, increasing to a 33.3% loss with 2" of steel. Since a minimum of 1" of steel was used on all tests, the application of the 16.7% will only be necessary to correct the four tests that were made with two 1" plates. This should provide comparable data on all targets.

As you may note, the entrance hole in the targets perforated through 2" of steel is smaller in diameter, a normal characteristic.

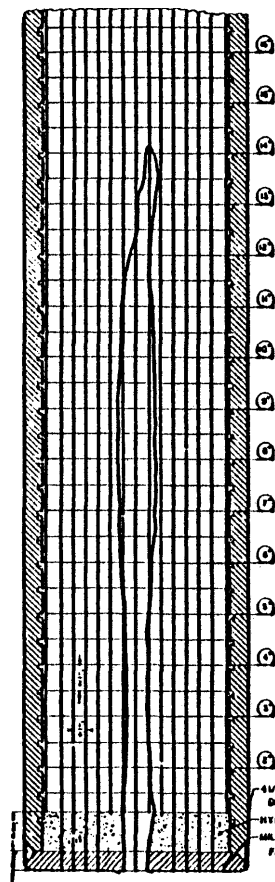
If you have any additional questions, please contact me.

Sincerely,


W. A. McPhee

WAM:lv
Enclosures

INDIVIDUAL SHOT RECORD
BEREA SANDSTONE CORE TARGET



100

API FORM 620

CERTIFICATION DATA SHEET

Service Company Dresser Atlas
 Gun (ID) and Designation 4" Konashot
 Charge Name NCE V Jumbo Jet
 Type Perforator Retrievable Hollow Carrier
 Recommended Minimum Pipe (ID) 6 1/2 in.
 Standard Gun Length 6 & 10 ft
 Maximum Gun One Run 188 shots
 Spacing Available 1, 2, 3, 4 shots ft
 Phasings Available 120 degree
 Firing Order Top down Yes Bottom up
 Available Firing Semi Selective Yes Simultaneous

Charge Weight 22.5 gm RDX powder
 Maximum 24 hour Temperature 350 F
 Maximum Pressure 20,000 psi
 Charge Case Material Rubber & Steel
 Carrier Material H. T. Steel
 Bullet (ID) _____ in, Length _____ in
 Debris Weight _____ gm charge
 Debris Description Debris contained in gun body
 Remarks Non-Carrot forming perforator

SECTION 1 - CONCRETE TARGET

Casing Data 6 1/2" OD 17 lb. ft. J55 API Grade
 Target Data 48 OD. Tensile Strength 453 psi. Compressive Strength 4642 psi
 Date of Test November 7, 1971 Age of Target _____ days

Shot No	No. 1	No. 2	No. 3	No. 4	No. 5	No. 6	Average
Clearance, in.	0	.88	.68	0	.68	.68	.45
Casing Hole Diameter, Short Axis, in.	.43	.34	.36	.35	.34	.31	.35
Casing Hole Diameter, Long Axis, in.	.44	.36	.37	.43	.36	.35	.40
Average Casing Hole Diameter, in.	.44	.36	.36	.39	.35	.33	.38
Total Depth, in.	19.05	20.05	19.43	18.93	19.05	20.93	19.57
Burr Height, in.	.08	.09	.10	.07	.10	.09	.09
Depth to Jet Debris of Bullet, in.	THE LINER USED IN THIS CHARGE IS NON-CARROT FORMING						

Remarks _____

SECTION 2 - BEREA SANDSTONE CORE TARGET

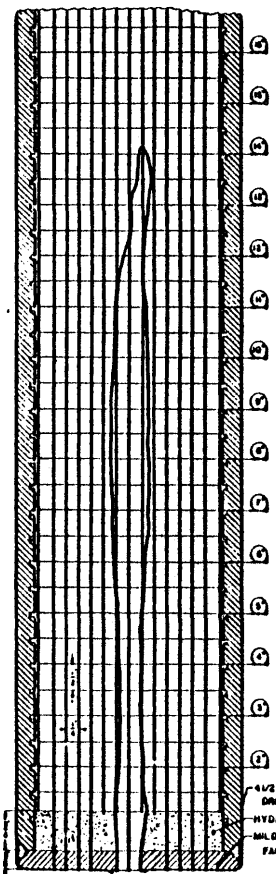
CORE DATA				SHOOTING CONDITIONS			FLOW CONDITIONS				RESULTS						
Test No	Test Date	Paraballs	S.	Core Length in.	A. mg	Pressure psi		Clearance in.	Pressure psi		Total Flow Mers	q _p mg	Entrance Hole Diam in.	LFL	HHP in.	ICP in.	LCP in.
						Well	Core Target		Well	Core Target							
1070	12-12-72	19.3	76.3	18	228	1500	1000	0.50	1000	1200	28	502	.44	.78	14.10	12.97	9.86
1071	12-16-72	19.2	74.4	21	160	1600	1000	0.50	1000	1200	31	304	.46	.85	14.00	12.87	10.93
1072	1-3-73	19.0	70.3	18	182	1500	1000	0.50	1000	1200	42	365	.43	.72	13.92	12.79	9.20
Average													.44	.78	14.01	12.88	10.00

I certify that these tests were made according to the procedures as outlined in API RP 13 Standard Procedure for Evaluation of Well Perforators, Second Edition, November 1971. All of the equipment used in these tests, such as the guns, jet charges, detonator cord, etc. was standard equipment with our company for use in the gas being tested, and was not changed in any manner for the test. Furthermore, the equipment was chosen at random from stock and therefore will be substantially the same as the equipment which would be furnished in perforate a well for any operator.

CERTIFIED BY [Signature] 3-1-77 Date
 Title V. P. Research & Engineering
 Address Houston, Texas

RECERTIFIED BY _____ Date _____
 Title _____ Address _____

INDIVIDUAL SHOT RECORD
BEREA SANDSTONE CORE TARGET



101

API FORM 430

CERTIFICATION DATA SHEET

Service Company Dresser Atlas
 Gun (ID) and Designation 4" Koneshot
 Charge Name 4 NCF V Jumbo Jet
 Type Perforator Retrievable Hollow Carrier
 Recommended Minimum Pipe (ID) 5 1/2"
 Standard Gun Length 8 & 10'
 Maximum Gun One Run 168 shots
 Spacing Available 1, 2, 3, 4' shots ft
 Phasings Available 120 degree
 Firing Order Semi Top down, Yes Bottom up
 Available Firing Selective, Yes Simultaneous

Charge Weight 22.5 gm RDX powder
 Maximum 24-hour Temperature 350 °F
 Maximum Pressure 20,000 psi
 Charge Case Material Rubber & Steel
 Carrier Material H. T. Steel
 Bullet (ID) _____ in., Length _____ in
 Debris Weight _____ gm charge
 Debris Description Debris contained in gun body.

Remarks Non-Carrot forming perforator

SECTION 1 - CONCRETE TARGET

Casing Data 5 1/2" (ID), 17 lb. ft., J-55 API Grade
 Target Data 48 (ID), Tensile Strength 453 psi, Compressive Strength 4842 psi
 Date of Test November 7, 1971 Age of Target _____ days

Shot No	No. 1	No. 2	No. 3	No. 4	No. 5	No. 6	Average
Clearance, in.	0	.88	.68	0	.68	.88	.45
Casing Hole Diameter, Short Axis, in.	.43	.34	.36	.36	.34	.31	.35
Casing Hole Diameter, Long Axis, in.	.44	.36	.37	.43	.36	.35	.40
Average Casing Hole Diameter, in.	.44	.36	.36	.39	.36	.33	.38
Total Depth, in.	19.05	20.05	19.43	18.93	19.05	20.93	19.57
Burr Height, in.	.08	.06	.10	.07	.10	.09	.09

Depth to Jet Debris or Bullet, in. _____
 Remarks THE LINER USED IN THIS CHARGE IS NON-CARROT FORMING

SECTION 2 - BEREA SANDSTONE CORE TARGET

CORE DATA						SHOOTING CONDITIONS			FLOW CONDITIONS				RESULTS				
Test No	Test Date	Porosity %	N ₂	Core Length in.	A, in.	Pressure psi		Clearance in.	Pressure psi		Total Flow Mscf	q _p md	Entrance Hole Diam in.	L/D	IIP in.	LIP in.	ECP in.
						Well	Core Target		Well	Core Target							
1070	12-12-72	19.3	78.3	18	228	1500	1000	0.50	1000	1200	28	602	.44	.76	14.10	12.97	9.86
1071	12-16-72	19.2	74.4	21	160	1500	1000	0.50	1000	1200	31	304	.46	.85	14.00	12.97	10.93
1072	1-3-73	19.0	70.3	18	182	1500	1000	0.50	1000	1200	42	365	.47	.72	13.92	12.79	9.20
Average													.44	.78	14.01	12.88	10.00

CERTIFICATION

I certify that these tests were made according to the procedures as outlined in API RP 43 Standard Procedure for Evaluation of Well Perforators, Second Edition, November 1971. All of the equipment used in these tests, such as the gun, jet charges, detonator cord etc., was standard equipment with our company for use in the gun being tested, and was not

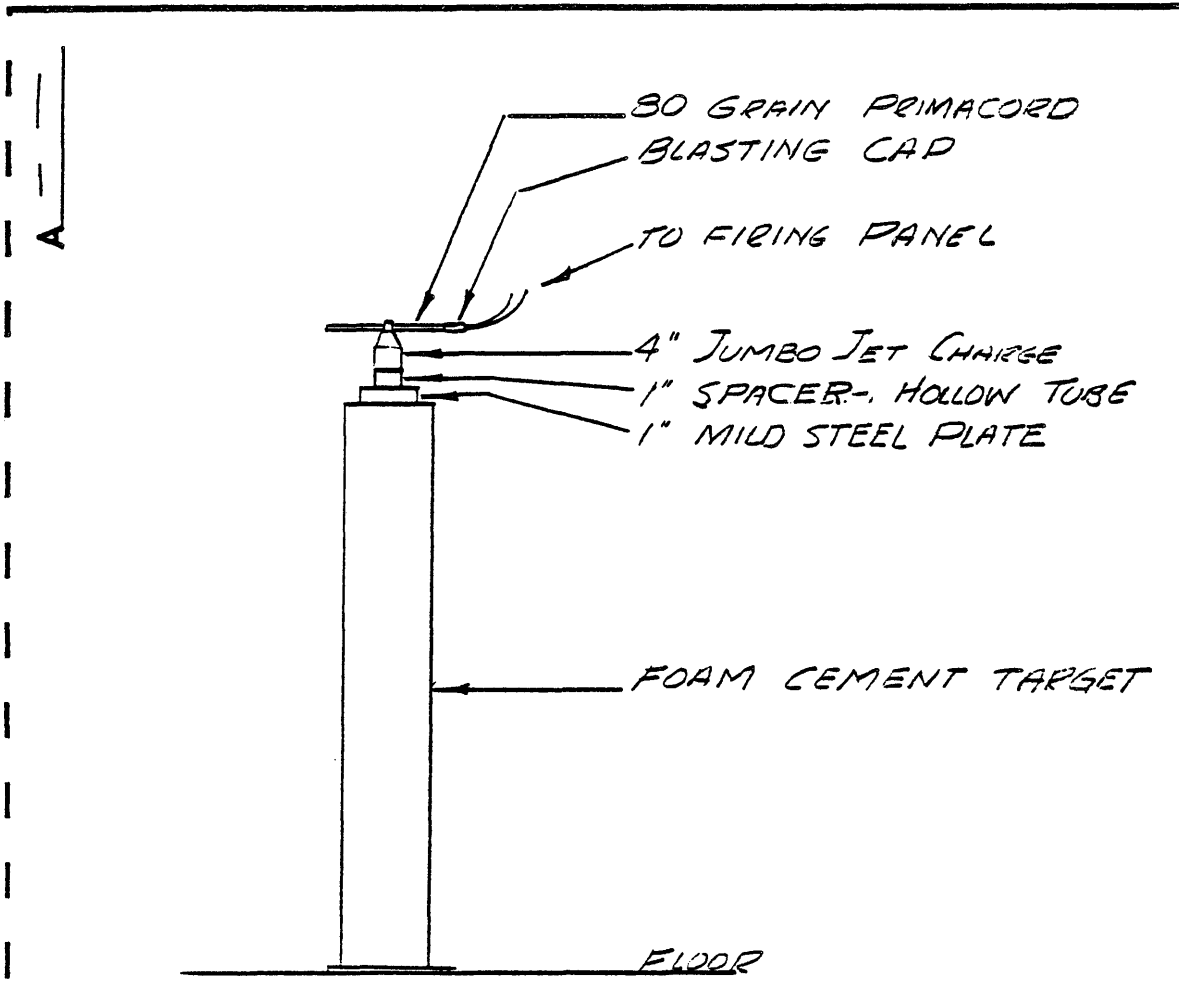
changed in any manner for the test. Furthermore, the equipment was chosen at random from stock and therefore will be substantially the same as the equipment which would be furnished to perforate a well for any operator.

CERTIFIED BY [Signature] 3-1-77
 Date _____
 RECHECKED BY _____
 Date _____

V. P. Research & Engineering
 Title _____
 Title (the reverse side) _____

Houston, Texas
 Address _____
 Address _____

4 1/2" IN. M. 60-LB/FT
 DRILL PIPE
 HYDROMITE - CM
 MIL-D-STEEL
 FACE PLATE



COLORADO SCHOOL OF MINES - KHALED CHERKERI

REV.	ECO No.	DESCRIPTION	(ZONE)	BY	APPD	DATE
CONFIDENTIAL		RELEASED TO AND ACCEPTED BY THE POSSESSOR ON CONDITION THAT NO RIGHTS OF REPRODUCTION OR USE ARE GIVEN EXCEPT FOR PURPOSES ELSEWHERE SPECIFIED IN WRITING BY DRESSER ATLAS.				
DO NOT SCALE PRINTS REMOVE BURRS AND SHARP EDGES LIMITS UNLESS OTHERWISE SPECIFIED		DR BY WAM	DATE 7/2/78	SERIES	ITEM	NEXT ASS'Y.
.000 ± .005 .00 ± .010 ± .05 SCALE		CHK				
CONCENTRICITY .005 T.I.R. ANGLES ± ½ DEG. MACHINED FINISH 125 ✓		ENGR				
		APPD				
		STDS				
Dresser Atlas						TITLE FOAM CEMENT TEST SETUP
RAW MAT'L	MATERIAL NO.	DESCRIPTION	HEAT TREAT	BILL MAT'L	DRAWING NUMBER	REV.
				<input type="checkbox"/>	_____	